SYNTHESIS, CHARACTERIZATION AND STUDY ON THE SORPTION PROPERTY OF $Fe_3O_4/Al_2O_3/ZrO_2$ NANOCOMPOSITES TOWARD THE REMOVAL OF CADMIUM, LEAD AND CHROMIUM IONS FROM AQUEOUS SOLUTION

MSc THESIS

FEKADU TSEGAYE DAJAN

OCTOBER 2016

HARAMAYA UNIVERSITY, HARAMAYA

Synthesis, Characterization and Study on the Sorption Property of $Fe_3O_4/Al_2O_3/ZrO_2$ Nanocomposites toward the Removal of Cadmium, Lead and Chromium from Aqueous Solution

A Thesis Submitted to the Department of Chemistry, Postgraduate Program Directorate

HARAMAYA UNIVERSITY

In Partial Fulfillment of the Requirements for the Degree of MASTER OF SCIENCE IN CHEMISTRY (ANALYTICAL CHEMISTRY)

Fekadu Tsegaye Dajan

October 2016

Haramaya University, Haramaya

HARAMAYA UNIVERSITY

POSTGRADUATE PROGRAM DIRECTORATE

As thesis research advisors, we hereby certify that we have read and evaluated this thesis prepared, under our guidance, by Fekadu Tsegaye entitled: "**SYNTHESIS, CHARACTERIZATION AND SORPTION PROPERTY STUDY OF $Fe_3O_4/Al_2O_3/ZrO_2$ NANOCOMPOSITES FOR THE REMOVAL OF CADMIUM, LEAD AND CHROMIUM FROM AQUEOUS SOLUTION"** We recommend that it be submitted as fulfilling the thesis requirement.

Dr. Abi Taddesse	_____	_____
Major Adivisor	Signature	Date
Dr. Endale Teju	_____	_____
Co-Advisor	Signature	Date
Prof. Isabel Diaz	_____	_____
Co-Advisor	Signature	Date

As members of the board of examiners of the MSc thesis open defense examination, we certify that we have read and evaluated the thesis prepared by Fekadu Tsegaye and examined the candidate. We recommended that the thesis be accepted as fulfilling the thesis requirement for the degree of Master of Science in Chemistry.

_____	_____	_____
ChairPerson	Signature	Date
_____	_____	_____
Internal Examiner	Signature	Date
_____	_____	_____
External Examiner	Signature	Date

DEDICATION

This thesis is dedicated to my mother **Bizunesh Gudeta,** my father **Tsegaye Dajan** and my Aunt **Jemanesh Gudeta** who encouraged and strengthened me in all my life**.**

STATEMENT OF THE AUTHOR

By my signature below, I declare and affirm that this Thesis is my own work. I have followed all ethical and technical principles of scholarship in the preparation, data collection, data analysis and compilation of this Thesis. Any scholarly matter that is included in the Thesis has been given recognition through citation.

This Thesis has been submitted in partial fulfillment of the requirements for an MSc degree in analytical chemistry at the Haramaya University. The Thesis is deposited in the Haramaya University Library and is made available to borrowers under the rules of the Library. I solemnly declared that this Thesis has not been submitted to any other institution anywhere for the award of any academic degree, diploma, or certificate.

Brief quotation from this Thesis may be made without special permission provided that accurate and complete acknowledgement of source is made. Requests for permission for extended quotation from or reproduction of this Thesis in whole or in part may be granted by the Director for Postgraduate Program Directorate or the Head of Chemistry Department when in his or her judgment the proposed use of the material is in the interest of scholarship. In all other instances, however, permission must be obtained from the author of the Thesis.

Name: **FEKADU TSEGAYE** **Signature** _____

Department: **Chemistry**

Date of submission: _____

ACRONYMS AND ABBREVATION

FAAS	Flame Atomic Absorption Spectrometry
FTIR	Fourier Transforms Infrared
XRD	X-ray Diffractometer
BET	Brunauer-Emmett-Teller
WHO	World Health Organization

BIOGRAPHICAL SKETCH

The author was born in November, 1991 at Girmi, East Shewa Zone, Oromia Region, Ethiopia. He attended his primary education in Gorogoro and Hama Primary School and his secondary school in Chafe Donsa and Bishoftu Secondary High Schools. After completion of his secondary school education, he joined Haramaya University in October, 2010 and graduated with BSc degree in Applied Chemistry in 2012. After graduation, he was employed as a graduate assistant in Hramaya University and then he joined the Postgraduate Program Directorate of Haramaya University in September, 2015 to pursue his MSc study in Chemistry (Analytical Chemistry).

ACKNOWLEDGEMENTS

First of all I would like to praise the Almighty God and His Mother St. Marry for bestowing up on me health, strength, patience and protection throughout the study period.

Secondly I would like to express my deepest gratitude to my advisors Dr. Abi Taddesse, Dr. Endale Teju and Prof. Isabel Diaz for their unreserved constructive advice, useful discussion, continuous guidance, friendly treatment, appreciable encouragement, visit to my laboratory work and carful supervision of my thesis research work.

I would also like to extend my heartfelt thanks to my mentor, Dr. Nigussie Bussa lecturer at Haramaya University, for his personal and professional support throughout my thesis research work and Haramaya University for giving me the opportunity to pursue my education and providing me financial support to accomplish the thesis work.

I would like to extend my gratitude to all my family members for their unreserved moral and financial support.

Last but not least, my heartfelt thanks also go to my colleagues and friends for their generous support and contribution for timely accomplishment of this work.

TABLE OF CONTENTS

LIST OF TABLES

Table **Page**

LIST OF FIGURES

Figure **Page**

LIST OF TABLES IN THE APPENDIX

Appendix table **Page**

LIST OF FIGURES IN THE APPENDIX

Appendix Figure **Page**

SYNTHESIS, CHARACTERIZATION AND STUDY ON THE SORPTION PROPERTY OF $Fe_3O_4/AL_2O_3/ZrO_2$ NANOCOMPOSITES TOWARD THE REMOVAL OF CADMIUM, LEAD AND CHROMIUM FROM AQUEOUS SOLUTION

ABSTRACT

The pollution caused by heavy metals is one of the major environmental problems that is imperative to be solved. Fe-Al-Zr ternary mixed oxides nanocomposite was Synthesized by using ferric chloride hexa hydrate, ferrous chloride tetrahydrate, aluminum nitrate nanohydrate and zirconyl chloride octahydrate via co-precipitate method. The crystallinity, surface area and functional group of the material were investigated by means of X-ray diffraction (XRD), Brunauer-Emmett-Teller (BET) and Fourier transform infrared (FTIR) techniques. The pH of point zero charge and ion strength of the selected adsorbent was also determined. The sorption kinetics and thermodynamics, the influence of some factors such as pH, adsorbent dose, contact time, speed of agitation and initial metal concentration on sorption were also investigated. The sorption properties of the adsorbent are also described. The results of batch sorption experiments in the determination of Pb(II), Cd(II) and Cr(VI) metal ion sorption behaviors and sorption mechanisms were presented and discussed. The effects of each of the above mentioned parameters on the adsorption of Pb(II), Cd(II) and Cr(VI) were determined to be pH = 6, dose = 1g, contact time = 12 h, agitation speed = 120 rpm with initial concentration of 20 ppm for Cd(II); pH = 4, dose = 0.1 g, contact time = 12 h, agitation speed = 120 rpm with initial concentration of 20 ppm for Cr(VI) and also pH = 6, dose = 0.5 g, contact time = 6 h, agitation speed = 100 rpm with initial concentration of 20 ppm for Pb(II) by Fe-Al-Zr. The experimental results showed that the adsorbed amounts of Pb(II), Cd(II) and Cr(VI) tend to decrease with increase in pH. Desorbabilty of Cd(II), Cr(VI) and Pb(II) was investigated and found to be increased with increasing pH. Freundlich isotherm models fit the equilibrium data well on the adsorbent. Kinetic data correlated well with the pseudo second order kinetic model, suggesting that more of the adsorption process might be chemical sorption. Since the value of the thermodynamics parameter (ΔG) appeared to be negative, the spontaneous nature of the adsorption process was confirmed. It has been found that, having all parameters optimized, the nanosized adsorbent entitled to have an adsorption efficiency of 96.65%, 96.55% and 97.2% for Cd(II), Cr(VI) and Pb(II), respectively. The effect of interfering cations on the adsorption of Cd(II), Cr(VI) and Pb(II) these also studied. Experimental results show that the nanocomposite was effective for the removal of the title heavy metals from aqueous solution.

Key word: Adsorption, co-precipitate, Nanocomposite, Point of Zero Charge.

1. INTRODUCTION

Heavy metals pollution represents a serious problem for human health and for life in general. The disposal of heavy metals is a consequence of several activities like chemical manufacturing, painting and coating, mining, extractive metallurgy, nuclear and other industries. Those metals exert a deleterious effect on fauna and flora of lakes and streams (Cristina *et al.,* 2009). Most of the heavy metals are toxic and due to their non- biodegradability and persistence, they tend to accumulate in living organisms causing various diseases and disorders. Ni, Cd, Hg, Zn, Pb and Cr are examples of metals that are harmful wastes produced by industries which pose a risk of contaminating groundwater and other water resources (Amiri *et al.,* 2014).

Among different heavy metals Chromium is one of the contaminants which exists in hexavalent and trivalent forms. Trivalent chromium is an essential element in human nutrition and is much less toxic than the hexavalent one, which is recognized as a carcinogenic and mutagenic agent. Chromium compounds are widely used by different industries such as metal plating, paints and pigments, leather tanning, textile dyeing, printing inks and wood preservation, so huge quantity of wastewater containing chromium is discharged into the environment. Therefore, removal of Cr(VI) from wastewater is essential before disposal (Mina *et al.,* 2011).

Cadmium (Cd) is a toxic heavy metal of significant environmental and occupational concern (Waalkes, 2000). It is introduced into water from smelting, metal plating, cadmium nickel batteries, phosphate fertilizers, mining, pigments, stabilizers, alloy industries and sewage sludge (Kadirvelu and Namasivayam, 2000). Contamination of drinking-water may occur as a result of the presence of cadmium as an impurity in the zinc galvanized pipes or cadmium-containing solders in fittings, water heaters, water coolers and taps.

Cadmium has been classified as a human carcinogen and teratogen, impacting the lungs, kidneys, liver and reproductive organs (Sharma, 2008; Waalkes, 2000). The harmful effects of cadmium include a number of acute and chronic disorders, such as renal damage, emphysema, hypertension and testicular atrophy (Kadirvelu and Namasivayam, 2000). Hence, it is essential to remove Cd(II) from water and wastewater prior to transport to prevent cycling into the natural environment. The most important technologies employed to remove cadmium include chemical precipitation, electro flotation, ion exchange, reverse osmosis and adsorption onto activated

carbon (Poon, 1986). Adsorption has been developed as an efficient method for the removal of heavy metals from contaminated water and soil (Zeid *et al*., 2011).

Lead as a toxicologically relevant element has been brought into the environment by man in extreme amounts, despite its low geochemical mobility and has been distributed worldwide (Simone *et al*., 2012). Lead amounts in deep ocean waters is about 0.01-0.02 μg/L, but in surface ocean waters is 0.3 μg/L (Castro-González and Méndez-Armenta, 2008). Lead still has a number of important uses in the present day; from sheets for roofing to screens for X-rays and radioactive emissions. Like many other contaminants, lead is ubiquitous and can be found occurring as metallic lead, inorganic ions and salts (Harrison, 2001). Lead has no essential function in man. Lead poisons to human beings causes severe damage to the kidneys, nervous system, reproductive system, liver, and brain. Excess exposure to lead has been responsible for sterility, abortion, stillbirths, and neo-natal deaths.

Various treatment techniques are practiced for removal of these heavy metals from water and wastewaters. These techniques are adsorption, chemisorption; absorption and ion exchange (Fetter, 1999), reduction, ion exchange, evaporation, reverse osmosis, adsorption, chemical coagulation, and precipitation. Each technique has its own limitations. Most of these techniques suffer from limitations such as high capital and difficult operational methods and there are problems in disposing the residual metal slugs.

The adsorption method is generally opted for the tertiary treatment of water where small concentrations of the dissolved species are present due to its low cost-effective, high efficiency, and simple to operate for removing trace levels of heavy metal ions, adsorption technology is regarded as the most promising one to remove heavy metal ions from effluents among these techniques mentioned above (Wang *et al.,* 2012). The use of activated carbons to remove organic and inorganic pollutants from water is widely extended, because of their high surface area, microporous character, and the chemical nature of their surface.

Adsorption is a process that occurs when a gas or liquid solute accumulates on the surface of a solid or a liquid (adsorbent), forming a molecular or atomic film (the adsorbate). Adsorption is operative in most natural physical, biological, and chemical systems, and is widely used in

industrial applications. Adsorption is currently considered to be very suitable for wastewater treatment because of its simplicity and cost effectiveness (Yadanaparthi *et al.,* 2009, Kwon *et al.,* 2010). Adsorption is commonly used technique for the removal of metal ions from various industrial effluents (Gottipati *et al.,* 2012).

Several heavy metals removing methods from groundwater remediation have been proposed including nanosized ferric oxides, zirconium oxides, aluminum oxides and application of mixed ferrous/ferric iron hydroxides. Nowday, many research groups have explored several nanoparticles for removal heavy metals, because of the ease of modifying their surface functionality and their high surface area to-volume ratio for increased adsorption capacity and efficiency. In the last decade, magnetic nanoparticle (MNP) adsorption has attracted much interest and is an effective and widely used process because of its simplicity and easy operation (Chanani *et al.,* 2015). Recently the magnetic nanoparticles exhibit amphoteric surface activity, easy dispersion ability and, to their very small dimensions, a high surface-to-volume ratio, resulting in a high metal adsorption capacity (Giraldo *et al.,* 2013), small size and magnetic property.

However, up to now no information is available on heavy metal removal by (Fe-Al-Zr) ternary nanocomposite, therefore, due to high surface area of Fe-Al mixed oxides and important scavenging property of Zr oxides and the magnetic nanoparticles(Fe_3O_4) exhibit a high surface-to-volume ratio, resulting in a high metal adsorption capacity and small size and magnetic. we are motivated to carry out experiment on the adsorption of the as-synthesized magnetic Fe-Al-Zr ternary nanocomposite for chromium, cadmium and lead in aqueous solution. Our aim was to synthesize multi-component oxide ($Fe_3O_4/Al_2O_3/ZrO_2$) surface which could increase the degree of elimination of these heavy metals from aqueous solution.

In the present study, a new magnetic ternary nanocomposite ($Fe_3O_4/Al_2O_3/ZrO_2$) was synthesized using co-precipitation method due to some important advantages of this method such as low reaction temperature, fine and uniform particle size with non-agglomerate or weakly agglomerate particles, easy scale-up and low cost, and time saving processing.

Objectives

General Objective:

The general objective of this study was to:

- Evaluate cadmium, chromium and lead removal efficiency by $Fe_3O_4/Al_2O_3/ZrO_2$ nanocomposite sorbent from aqueous solution.

Specific Objectives:

The specific objectives of this study were:

- To synthesize $Fe_3O_4/Al_2O_3/ZrO_2$ nanocomposite by co-precipitation method.
- To characterize the as synthesized nanosorbent by using modern techniques such as FTIR, XRD, BET, and FAAS.
- To remove chromium, cadmium and lead from aqueous solution by selective adsorption on synthesized nanosorbent.
- To determine the effect of experimental parameters on the adsorption of the three metals on the as-synthesised sorbent.
- To evaluate the adsorption process by using the Langmuir, Freundlich, thermodynamic and kinetic.
- To evaluate the extent of desorption and recyclability of the nanosorbnet.

2. LITERATURE REVIEW

2.1. Heavy Metals

Heavy metals are elements having atomic weights between *63.5* and 200.6 g/mol, and a specific gravity greater than *5.0.* Most of the heavy metals are dangerous to health or to the environment (Dimple, 2014). Heavy metals include lead (Pb), cadmium (Cd), zinc (Zn), mercury (Hg), arsenic (As), silver (Ag) chromium (Cr), copper (Cu) iron (Fe) and the platinum group elements (Duruibe *et al.*, 2007). The major toxic metals are Cd, Zn, Pb and Ni. These heavy toxic metals enter the water bodies through waste water from metal plating industries and mining, pigments and alloys, electroplating corrosion of galvanized piping and dezincification of brass besides other industrial wastes (Mousavi *et al.*, 2010).

Different contaminants are released to wastewater with the rapid industrialization of human society, including heavy metal ions, organics, bacteria, viruses, and so on, which are serious harmful to human health. Among all water contaminations, heavy metal ions, such as Pb^{2+}, Cd^{2+}, Zn^{2+}, Ni^{2+} and Hg^{2+}, have high toxic and nonbiodegradable properties, can cause severe health problems in animals and human beings. It is well-known that chronic cadmium toxicity is the inducement of Japan Itai-Itai disease. The harmful effects of cadmium (Cd) also lead (Pb) a number of acute and chronic disorders, such as renal damage, emphysema, hypertension, testicular atrophy, and skeletal malformation in fetus. Wastewater from many industries, including chemical manufacturing, battery manufacturing industries, metallurgical, leather tanning, and mining, contain these heavy metal ions. These wastewater with heavy metal ions are discharged into natural water directly, not only threat the aquatic organisms, but may be enriched by precipitation, adsorption, and harmed human health through the food chain. Thus, the removal of such toxic metal ions from wastewater is becoming a crucial issue (Wang *et al.,* 2012)

2.1.1. Lead

Lead contamination of the environment is primarily due to anthropogenic activities, making it the most ubiquitous toxic metal in the environment. Lead readily accumulates in the humus rich surface layer of the soils due to its complexity with organic matter and it was reported to be the least mobile heavy metal in soils under reducing and non-reducing conditions. Lead has been

implicated to be the most common heavy metal contaminants in urban soils due to atmospheric deposition from automobile emission and industries (Abdus-salam and Adekola, 2005).

Lead enters man by inhalation and ingestion. Absorbed and carried by the blood, accumulated in liver, kidney, and bone up to about the fifth decade of life. Lead causes brain damage particularly to the young. There is evidence that Lead pollution can induce aggressive behavior in animals which can also occur in humans (Mengel and Kirkby, 1978).

2.1.2. Cadmium

The use of cadmium by man is relatively recent and it is only with its increasing technological use in the last few decades that serious consideration has been given to cadmium as a possible contaminant. Cadmium is naturally present in the environment: in air, soils, sediments and even in unpolluted seawater. Cadmium is emitted to air by mines, metal smelters and industries using cadmium compounds for alloys, batteries, pigments and in plastics, although many countries have stringent controls in place on such emissions (Harrison, 2001).

Cadmium is a highly toxic inorganic pollutant whose emission sources are widely diffused, giving rise to a large scale environmental pollution. For these reasons, environmental regulations define severe limitations on the maximum cadmium concentration in natural water bodies as well as on the maximum allowed concentration for wastewater discharge.

Tobacco smoke is one of the largest single sources of cadmium exposure in humans. Tobacco in all of its forms contains appreciable amounts of the metal. Because the absorption of cadmium from the lungs is much greater than from the gastrointestinal tract, smoking contributes significantly to the total body burden (Ming-Ho, 2005; Figueroa, 2008).

Cadmium accumulates in the human body affecting negatively several organs: liver, kidney, lung, bones, placenta, brain and the central nervous system. Other damages that have been observed include reproductive, and development toxicity, hepatic, haematological and immunological effects (Simone *et al.,* 2012).

2.1.3. Chromium

Chromium is one of the contaminants which exist in hexavalent and trivalent forms. Trivalent chromium is an essential element in human nutrition and is much less toxic than the hexavalent one, which is recognized as a carcinogenic and mutagenic agent. Chromium compounds are widely used by different industries such as metal plating, paints and pigments, leather tanning, textile dyeing, printing inks and wood preservation, so huge quantity of wastewater containing chromium is discharged into the environment. Therefore, removal of Cr(VI) from wastewater is essential before disposal (Mina *et al.,* 2011).

Cr(VI) is a toxic metal and on the list of priority pollutants due to its mutagenic and carcinogenic properties deûned by the US EPA (Environmental Protection Agency). Chromium exists in either +3 or +6 oxidation states, as all other oxidation states are not stable in aqueous systems. Chromium (VI) is 100-1000 times more toxic to organisms than Cr(III) and more readily transported in soils. Cr(VI) is mainly from electroplating, leather tanning, textile dyeing and metal finishing industries. The US EPA requires Cr(VI) in drinking water and inland surface waters is 0.05 and 0.1 mg/L, respectively (Amiri *et al.,* 2014).

Cr(VI) has been demonstrated to have a number of adverse effects ranging from irritation to causing cancer. Effects in humans occupationally exposed to high levels of chromium compounds, primarily Cr (VI) by inhalation, may include irritating respiratory effects, effects on stomach and blood, liver and kidney effects, and increased risk of death from lung cancer.Evidence from studies on experimental animals' shows that Cr(VI), especially those of low solubility, can induce lung cancer. Trivalent chromium is not considered to be carcinogenic (David *et al.,* 2008).

2.2. Nanotechnology

Nanotechnology is a field of applied science, focused on the design, synthesis, characterization and application of materials and devices on the nanoscale. It is an emerging field that covers a wide range of technologies which are presently under development in nanoscale. It plays a major role in the development of innovative methods to produce new products, to substitute existing production equipment and to reformulate new materials and chemicals with improved

performance resulting in less consumption of energy and materials and reduced harm to the environment as well as environmental remediation (Mansoori *et al.,* 2008). As the exciting field of nanotechnology develops, the broader environmental impacts of nanotechnology will also need to be considered. Such considerations might include: the environmental implications of the cost, size and availability of advanced technological devices; models to determine potential benefits of reduction or prevention of pollutants from environmental sources.

Pollution prevention by nanotechnology refers on the one hand to a reduction in the use of raw materials, water or other resources and the elimination or reduction of waste and on the other hand to more efficient use of energy or involvement in energy production (USEPAR, 2007).

2.2.1. Application of Nanoparticles

Metal oxide nanoparticles are attractive for a large variety of applications including catalysis, sensors, (opto) electronic materials, and environmental remediation (Oskam, 2006) a semiconductor, electroluminescent or thermoelectric material, but they are also used in biomedical applications as drug delivery systems for treatment and diagnosis and in environmental decontamination applications (Haddad and Seabra, 2012; Corr, 2013).

A particle in physics can be defined as a tiny object, particularly localized object, that different chemical and physical properties can be attributed to it (Kuchibhatla *et al., 2007*). Particles can be found in different sizes and shapes. The word 'nano' comes from the Greek word 'nanos '(Suryanarayana, 2002*)*, refers to small animal or plant. Nano represents the number 10^{-9} i.e., one billionth of any unit. 1nm nanometer is 10^{-9} meter. In nanotechnology a particle is a unit of material which behaves as a whole regarding chemical and physical properties (Kuchibhatla *et al.,* 2007; Suryanarayana, 2002). Particles can be divided in different categories based on their size. Particles over 2500 nm are called coarse particles while particles with the size range of 100-2500 nm are named fine particles. Coarse particles are totally out of this research interests. Particles in the size range of 1-100 nm are specifically addressed as nanoparticles. Particles over 100 nm up to 1 micron can still be called nanoparticles but mainly when it is said nanoparticles, 1-100 nm is meant (Suryanarayana, 1995; Suryanarayana, 2002).

Nanoparticles have a large functional surface which is able to bind, adsorb and carry other compounds such as drugs, probes and proteins. On the other hand, nanoparticles have a surface that might be chemically more reactive compared to their fine analogues (Borm and Wolfgang, 2004). For example iron nanoparticles have been shown to be effective in the transformation, detoxification and/or sorption of a wide variety of common environmental contaminants, such as chlorinated organic solvents, organochlorine pesticides, and polychlorinated biphenyls (Zhang, 2003; USEPAR, 2007). Immobilizing nanoparticles onto a bulk carrier can, however, prevent their release into the environment whilst maintaining their reactivity. A number of water remediation devices have been developed based on iron nanoparticles immobilized into polymer matrices, which are usually produced as beads or fibers (Vatutsina *et al* ., 2007).

2.2.2. Mixed Oxide Nanoparticles

Magnetic nanoparticles have applications in information storage, magnetic refrigeration, (Michael *et al.,* 1992) medical diagnosis, (Josephson *et al.,* 1999). Controlled drug delivery, and as ferrofluids. Thus, developing a new synthetic route for magnetic nanoparticles and the investigation of their properties are of great importance (Shafi, 2002). Nanocrystal materials are also known to have superior mechanical properties due to the extremely fine grain size. However, it has not been well established that alloy and alloy-oxide composite coatings with nanocrystal grains have unique properties at high temperatures. Nanocrystal structures promote selective oxidation, forming protective oxidation scales with superior adhesion to the substrate.

Nano- Fe_3O_4 find applications as (a) Wave-absorbing Materials Fe_3O_4 is highly absorbent of magnetic waves and thus can be used in military high- performance micro meter and millimeter stealth materials, visible light-IR stealth materials, constructive stealth materials and radiation shielding materials for cell phones.(b)Paste for Inducing Magnetism due to its high saturated magnetic strength and high magnetic induce ratio, Fe_3O_4 can be made into paste for inducing magnetism to be used in adhesive structures of very fine magnetic heads. (c) Magnetic Fluid due to it's excellence in producing magnetic fluid, Fe_3O_4 can be widely used in sealing, anti-shock, medical instruments and equipment, volume tuning, light displaying, etc.(d)Adsorbent Nanotechnology is also involved in the removal of toxic metal pollutants from waste water. Industrialization has brought about an ever-increasing exposure to toxic heavy metals such as

lead, mercury or arsenic where they are irresponsibly dumped into rivers and oceans. A process using iron oxide nano particles as adsorbent to attract these heavy metals has been developed. It has been widely used in a variety of technological applications, such as a catalyst for ammonia, ceramics, energy storage, magnetic data storage, ferrofluids, and bioapplications. Keeping view of applications and importance of nano Fe_3O_4 in diversified fields,we synthesized magnetite by one of the cheap and convenient method (Kulkarni *et al.,* 2012).

Ferrites, the transition metal oxides having a spinal structure, are technologically important because of their interesting magnetic and electrical properties. They are used in magnetic inks and magnetic fluids, and for the fabrication of magnetic cores of read/write heads for high-speed digital tapes or for disc recording (Charles *et al.,* 1980). One important example is manganese oxide, which has the desirable properties of low cost and low toxicity. As with other electrically conductive metal oxides, manganese oxide stores electrical charge by a double insertion of electrons and cations into the solid state.

Maghemite (γ-Fe_2O_3, the ferromagnetic cubic form of iron (III) oxide) is also technologically important, as it is being used widely for the production of magnetic materials and catalysts. Because of the small coactivity of Fe_2O_3 nanoparticles, which arises from a negligible barrier in the hysteresis of the magnetization loop, they can be used as magneto-optical devices. Magneto-optic media can be made by depositing magnetic and optically transparent materials, and maghemite particles satisfy this condition, since they can be easily incorporated in to ultrathin polymer films. In this paper, we discuss the sonochemical synthesis and characterization of nanosized manganese iron oxide powder.

2.3. Sorption Processes

2.3.1. Definition

Sorption is a generic term with a variety of definitions. Sorption generally refers to processes describing the accumulation of a solute of interest at the interface solid and the aqueous phase. It includes adsorption, chemisorption; absorption and ion exchange (Fetter, 1999) expand this definition to include processes such as surface precipitation and diffusion of solutes into porous media. According to sorption is any process at the interface (solid-liquid) leading to solute phase

change or to solute/its environment induced surface transformation. The associated mechanisms are ion exchange, surface complexation, surface precipitation, hydrophobic controlled sorption, absorption, and diffusion in the solid phase. Sorption of U (VI) onto mineral surfaces has the tendency to increase with increasing pH, (up to pH = 7). This process however, is reversible when pH decreases.

2.3.2. Adsorption

Adsorption is the process through which a substance, originally present in one phase, is removed from that phase by accumulation at the interface between that phase and a separate (solid) phase. In principle adsorption can occur at any solid fluid interface. Examples include: liquid-solid interface (as in the adsorption of uranium on Iron/Alumina/Zirconium Mixed Oxide Sorbent System). Adsorbate or solute: the material being adsorbed (e.g., uranium solution). Adsorbent: the solid material being used as the adsorbing phase (e.g., Iron/Alumina/Zirconium Mixed Oxide). Adsorption the fixation of solute at the surface of the solid. However, the terms fixation, adherence, uptake, retention, accumulation and sorption are used interchangeably referring to any process leading to the removal of the metal/metalloid of interest from the aqueous phase. Thus, the term sorption in this study refers to all of the mechanisms listed by Fetter (1999).

2.3.3. Fundamentals of Adsorption

Adsorption is a mass transfer process in which substances present in a liquid phase are accumulated on a solid phase and thus removed from the liquid. Whereas absorption means that the molecules are accumulated in the phase, in adsorption the accumulation takes place at the boundary layer between solid and liquid phase. The solid phase onto whose surface the target compound is adsorbed is referred to as the adsorbent. The target compound (e.g., uranium) is called the adsorbate (Ingrid and Jamie, 1999) during the adsorption process; dissolved species are transported into the porous adsorbent particle by diffusion and are then adsorbed onto the extensive inner surface of the adsorbent.

Depending on the type of interaction between adsorbate and adsorbent surface, chemisorptions and physical adsorption can be differentiated. Chemisorption typically shows bonding energies

above 200kJ/mol. Here, the adsorbate reacts with the surface to form a covalent or an ionic bond. Physical adsorption is a rapid process caused by nonspecific binding mechanisms such as van der Waals forces and results in bonding energies of 4 - 40 kJ/mol. Generally, physical adsorption is less specific for which compounds adsorb to surface sites, has weaker forces and energies of bonding, operates over longer distances (multiple layers), and is more reversible (John *et al.,* 2005).

2.3.4. Freundlich Isotherm

This is commonly used to describe the adsorption characteristics for the heterogeneous surface. These data often fit the empirical equation proposed by Freundlich:

$$Q_{e=}K_e\ C_e^{\frac{1}{n}} \quad (1)$$

Where K_f= Freundlich isotherm constant (mg/g)
n = adsorption intensity;
Ce = the equilibrium concentration of adsorbate (mg/L)
Qe = the amount of metal adsorbed per gram of the adsorbent at equilibrium (mg/g).
Linearizing equation 1, we have:

$$\log Q_e = \log K_f + log\,\frac{1}{n} C_e \quad (2)$$

The constant K_f is an approximate indicator of adsorption capacity, while 1/n is a function of the strength of adsorption in the adsorption process. If n = 1 then the partition between the two phases are independent of the concentration. If value of 1/n is below one it indicates a normal adsorption. On the other hand, 1/n being above one indicates cooperative adsorption. The function has an asymptotic maximum as pressure increases without bound. As the temperature increases, the constants K_f and n change to reflect the empirical observation that the quantity adsorbed rises more slowly and higher pressures are required to saturate the surface. However, K_f and n are parameters characteristic of the sorbent-sorbate system, which must be determined by data fitting and whereas linear regression is generally used to determine the parameters of kinetic and isotherm models. Specifically, the linear least-squares method and the linearly transformed equations have been widely applied to correlate sorption data where 1/n is a

heterogeneity parameter, the smaller 1/n, the greater the expected heterogeneity. This expression reduces to a linear adsorption isotherm when 1/n = 1. If n lies between one and ten, this indicates a favorable sorption process (Dada *et al.,* 2012).

2.3.5. Langmuir Isotherm

The Langmuir adsorption isotherm is used to describe the equilibrium between surface and solution as a reversible chemical equilibrium between species (Langmuir, 1978). The adsorbent surface consists of fixed individual sites where adsorbate molecules can be chemically bound. It is assumed that the reaction has a constant free-energy change (ΔG_{ads}) for all sites and a maximum of one adsorbate molecule can be bound to each site (monolayer coverage). The following expression for the adsorption equilibrium capacity can be derived for liquids adsorbed on solids:

$$q_e = Q_o \frac{bC_e}{1+bC_e} \tag{3}$$

b is the ratio of adsorption and desorption rates and Q_o is the maximum uptake corresponding to the site saturation, indicating monolayer coverage. To derive the model parameters Q_o and b, the above equation can be linearized. The linear Langmuir isotherm allows the calculation of adsorption capacities and equated by the following equation.

$$\frac{C_e}{q_e} = \frac{1}{bQ_o} + \frac{C_e}{Q_o} \tag{4}$$

The Langmuir equation assumes a homogeneous structure of the adsorbent surface, i.e. all adsorption sites are energetically equal. That is why the Langmuir equation is in most cases only applicable for small concentration ranges.

2.4. Thermodynamic Study

The thermodynamics of metal ion sorption has been investigated extensively. Generally, there are two common types: endothermal and exothermal sorption processes. If the sorption increases with increasing temperature, it means that the sorption is an endothermal process. Whereas the sorption decreases with increasing temperature, indicates the exothermal sorption process. The

thermodynamic parameters such as free energy (ΔG^0), enthalpy (ΔH^0) and entropy changes (ΔS^0) for the sorption of Cu(II) were computed to predict the nature of sorption process. The removal of Cu(II) increased with increasing temperature. Negative values of ΔG^o indicate the feasibility of the process and spontaneous nature of the sorption with a high preference of Cu (II) for all adsorbents. Positive values of ΔH^o indicate the endothermic nature of the process, while positive values of ΔSo reflect the affinity of the adsorbents for Cu(II) ions and suggest some structural changes in adsorbate and adsorbent.

Thermodynamic parameters associated with adsorption, free energy change (ΔG), enthalpy change (ΔH) and entropy change (ΔS) will be calculated for the sorbent. By plotting the graph lnKc versus T-1, the values of ΔH and ΔS can be estimated from the slopes and intercepts hence spontaneity of the process will also be assessed by using the following equation:

$\Delta G = -nRT\ln Kc$
$\Delta G = \Delta H – T\Delta S$
$\ln K_c = \Delta S/R - \Delta H/RT$, Where: $\ln K_c = q_e/C_e$ (5)

Where R (8.314 J/mol K) is the gas constant, T(K) is the absolute temperature and K_c (cm^3g^{-1}) is the standard thermodynamic equilibrium constant defined by q_e/C_e. Thermodynamic considerations of an adsorption process are necessary to conclude whether the process is spontaneous or not. Gibb's free energy change, Δ*G*, is the fundamental criterion of spontaneity. Reactions occur spontaneously at a given temperature if Δ*G* is a negative value (Yohannes, 2014).

2.5. Kinetic Studies

Several kinetic models have been applied to examine the controlling mechanism of metal ion adsorption from aqueous solution. In this study pseudo-first order, pseudo-second order, and intra-particle diffusion were applied. Lagergren's first order rate equation is the earliest known to describe the adsorption rate based on adsorption capacity. The linear form of Lagergren's first order rate equation is as follows:

$$\ln(q_e - q_t) = \ln(q_e) - k_1 t \quad (6)$$

where qe is the amount of metal ion adsorbed onto the adsorbent at equilibrium (mg/g), q_t is the amount of metal ion adsorbed onto the adsorbent at any time t (mg/g), and K_1 (min^{-1}) is the rate

constant of the pseudo-first-order adsorption which can be calculated from the slope of the linear plot of $\ln(q_e - q_t)$ vs t. (slope = K_1, q_e = exp intercept).

Ho (1995) proposed a second order model for the sorption of divalent metal ions onto peat particles based on the adsorption capacity of the adsorbents with the goal of differentiating the kinetics of a second-order rate expression based on the adsorbent concentration from models which are based on the solute concentration and represent a pseudo-second-order rate expression. The linearized form of the pseudo-second-order model as given by Ho (1995) is

$$\frac{t}{q_t} = \frac{1}{K_2 q_e^2} + \left(\frac{1}{q_e}\right) t \tag{7}$$

Where K_2 ($gmg^{-1}min^{-1}$) is the rate constant of the pseudo-second-order adsorption, *qe* is the amount of metal ion adsorbed on the adsorbent at equilibrium (mg/g), and qt is the amount of metal ion adsorbed on the adsorbent at any time, *t* (mg/g). K_2 ($gmg^{-1}min^{-1}$) can be calculated from the slope and intercept of the plot of t/q_t against *t*. The intra-particle diffusion equation can be written as

$$q_t = K_{id} t^{0.5} + C \tag{9}$$

Where q_t is the amount of metal ion adsorbed onto the adsorbent at time *t* (mg/g), *C* is the intercept, and K_{id} is the intra-particle diffusion rate constant (mg g^{-1} min^{-1}) (Vijayakumar *et al.,* 2012).

2.6. Synthesis Techniques of Nanosorbent

There are many methods of synthesizing metal oxide nanoparticles. Among them some methods such as hydrothermal, (Yin *et al.,* 2001) microwave synthesis; sol-gel processing (Watson *et al.,* 2004) and co-preciptation methods are mostly used due to purity, homogeneity, ease of preparation and ease of introducing dopants.

2.6.1. Hydrothermal Synthesis Method

Hydrothermal synthesis is typically carried out in a pressurized vessel called an autoclave with the reaction in aqueous solution (Chen and Mao, 2007). The temperature in the autoclave can be

raised above the boiling point of water, reaching the pressure of vapor saturation. Hydrothermal synthesis is widely used for the preparation of metal oxide nanoparticles which can easily be obtained through hydrothermal treatment of peptised precipitates of a metal precursor with water (Chen and Mao, 2007). Hydrothermal method can be useful to control grain size, particle morphology, crystalline phase and surface chemistry through regulation of the solution composition, reaction temperature, pressure, solvent properties, additives and aging time (Carp *et al.,* 2004).

2.6.2. Sol-Gel Method

Sol-gel processing is a common chemical approach to produce high purity materials shaped as powders, thin film coatings, fibers, monoliths and self-supported bulk structures (Keshmiri *et al.,* 2006). The sol-gel method has several advantages over other synthesis techniques such as purity, homogeneity, ease of preparation and ease of introducing dopants, composition and the ability to produce thin film coatings or porous powders. There are two possible routes for carrying out sol-gel synthesis, the non-alkoxide route and the alkoxide route. This requires the removal of the inorganic anion to produce the required oxide. However, halides often remain in the final oxide material and are difficult to remove. The alkoxide route involves hydrolysis of a metal alkoxide, followed by condensation. The hydrolysis/condensation reactions typically form a three dimensional polymeric structure, that, upon calcination will result in an atase or rutile metal oxide crystals depending on the calcination temperature.

2.6.3. Co-precipitation Method

The co-precipitation method involves the separation of solid containing target metal ions from a solution phase. In the process of co-precipitation, the metal components of the superconducting materials are first dissolved in solution. The solution combines with the precipitants in the supersaturated condition to form ion associates or clusters. A homogeneous co-precipitation process results in the formation of crystal line or amorphous solids which depends upon the condition under which the precipitate has been formed, the individual characteristics of the particular substance and its aging after precipitation. The most important advantage of this technique is its feasibility for large-scale production as well as its simplicity and low cost (Yanjun*et al*., 2008). Co-precipitation method also offers some other advantages. They are:-

Simple and rapid preparation, Easy control of particle size and composition and Various possibilities to modify the particle surface state and overall homogeneity.

2.7. Desorption Process and Regeneration of Adsorbents

Regeneration of adsorbents and recovery of loaded pollutants are quite important in adsorption process. If adsorption is thought of as surface complexation reaction a high concentration of OH^- ions shifts the equilibrium so that less adsorbate is bound to the surface. Also the surface acid/base reaction is shifted more towards negatively charged species, which hinders adsorption of anions such as phosphate. Consequently, a pH increase due to the use of caustic agents such as NaOH shifts the adsorption equilibrium and can result in desorption of the adsorbed solute. If the adsorption capacity can be regained in this process, the adsorbent will be regenerated. In several studies, sodium hydroxide (NaOH) solution has been shown as suitable regenerant for metal oxide adsorbents as well as hybrid anion exchange resins. Lead adsorption behavior was not adversely affected by repeated adsorption/desorption cycles Almost no loss in capacity after up to 12 adsorption/ desorption cycles was reported. Recently developed hybrid anion exchangers containing hydrated ferric oxide nanoparticles were reported to remove lead and showed much higher capacities than the parent material. The metal desorbability was defined as:

$$\%\, Desorption\ efficiency\ = \frac{Desorbed}{Adsorbed}\ x\ 100 \qquad (10)$$

Where, Desorbed: the concentration of the lead ion after the desorption process and Adsorbed: (C_o–C_e) for each recovery process.

2.8. Effect of ionic strength

Ionic strength parameter is very important in the adsorption process of metal ions since high ionic strength solutions are similar to wastewaters and it can bring a different condition in adsorption which is as a result of electro-statistic interaction between metal ions and adsorbent surface. According to the surface chemistry theory explained by Guoy and Chapman, when solid adsorbent is contact with sorbent species in solution, they are bound to be surrounded by an electrical diffused double layer, the thickness of which is significantly expanded by the presence of electrolyte.

Recently, for investigating the effect of ionic strength on adsorption process by zinc oxide nanoparticles, the efficiency of three distinct ionic strengths (0.1, 0.3, and 3 mol/L) were selected and with an increase of ionic strength from 0.1 to 3 mol/L, cadmium removal efficiency decreased. The reason is that the concentration of Na ions increases in the solution as ionic strength of the solution increases. The Na ions are positioned adjacent to the surface of zinc oxide nanoparticles. The association of these positive ions around the adsorbent causes a decrease in the contact between cadmium and nanoparticles and at the end, cadmium adsorption potential by zinc oxide nanoparticles decreases. On the other hand, the high concentration of Na ions competes well with cadmium ions and set on the active sites present on the surface of nanoparticles. Consequently, the active sites on the surface of the zinc oxide nanoparticles saturate and bring about a decrease in cadmium removal efficiency. The ionic strength of the solution becomes 30 fold (from 0.1 to 3 mol/l) the removal efficiency decreases a little (from 90.7 to 72.1%). It illustrates that high concentration of Na ions cannot completely occupied active sites and an electrical diffused double layer occurs by Na ions that it cause a repulsion between ions in the solution (Salmani *et al.,* 2013).

3. MATERIALS AND METHODS

3.1. Experimental Site

Synthesis of the adsorbent, the batch adsorption experiments and elemental analysis were carried out at the Instrumental Laboratory of Chemistry Department and the Central Laboratory, Haramaya University. Characterization of the synthesized adsorbents by FTIR was performed at Addis Ababa University. Similary, characterizations using XRD and BET were carried out at the Institute of Catalysis and Petroleum Chemistry (CSIC), Madrid, Spain.

3.2. Apparatus and Instruments

The laboratory apparatus used during the study include, different sized glassware (beakers, volumetric & erlenmeyer flasks, cylinders, pipettes, droppers, digestion tube and funnel) filter paper, mortar & pestle, desiccator and thermometer.

Instruments such as pH meter (JENWAY 3310), Analytical balance (aeADAM, AFP-720L) rotary shaker (Orbital shaker SO1 made in UK), sonicator(Kerry), flame atomic absorption spectrophotometer (FAAS model 210 VGP Back Scientific made in U.S.A), deionizer (Wation DB 50), digital hot air oven (Sentwin, india), FT-IR, X-Ray diffractometer (XRD), and Brunauer–Emmett–Teller (BET).

3.3. Chemicals and Reagents

The chemicals and reagents include: ($K_2Cr_2O_7$) (99.5% Bulux, india), $Cd(NO_3)_2.4H_2O$ (98% Bulux),$Pb(NO_3)_2$ (99% Bulux, india), aluminum nitrate nanohydrate ($Al(NO_3)_3.9H_2O$) (98% Bulux, india), ferrous chloride tetrahydrate ($FeCl_2.4H_2O$) (99.7% Uni-Chem), ferric chloride hexahydrate ($FeCl_3.6H_2O$) (99% Bulux, india), Zirconyl chloride octahydrate ($ZrOCl_2.8H_2O$), sodium hydroxide (NaOH) (98% BDH), sodium chloride (NaCl) (99.8% Uni-Chem), potassium chloride (KCl) (99.5% Bulux, india), Magnesium chloride six hydrate ($MgCl_2.6H_2O$) (98% Uni-Chem), iron sulfate heptahydrate $FeSO_4.7H_2O$ (98.5- 104.5% Bulux, india) , Calcium carbonate ($CaCO_3$) (99.5% BDH), Sodium nitrate ($NaNO_3$) (98% BDH, England) and hydrochloric acid (HCl) (36-38% Finken) all analytical grade were used. The pH of the working solutions were regulated by addition of HCl or NaOH solution.

3.4. Experimental Procedures

3.4.1. Sample Preparation

Stock solution (1000 mg L^{-1}) of Cr(VI), Pb(II) and Cd(II) metal ions were prepared from $K_2Cr_2O_7$, $Pb(NO_3)_2$ and $Cd(NO_3)_2.4H_2O$ by dissolving appropriate amount in 250 mL of slightly acidified double distilled water, respectively. The working solutions of 100 mgL^{-1} of each were prepared daily by suitable dilution of the stock solutions.

3.4.2. Synthesis Procedure of the Adsorbent

The ternary oxide nanocomposite adsorbent was prepared by chemical co-precipitation method as reported by (Liyuan *et al.,* 2013) with additional modification. Stoechiometric factors of Fe^{2+} and Fe^{3+} are very important for magnetic property of the composite products. Fe^{2+}/Fe^{3+}mole ratio < 0.1 is too small to achieve a stable solution. Fe^{2+}/ Fe^{3+} mole ratio < 0.3 from two different phase FeO(OH) surface functional group and low Fe^{3+} content ≈ 0.07 and the second phase, increased Fe^{2+} content ≈ 0.33 . For 0.5 Fe^{2+}/ Fe^{3+} mole ratio of the product obtained was homogeneous magnetic particle with uniform size and composition. So, in all samples the mole ratio of Fe^{2+}/ Fe^{3+} was selected to be 0.5 (Anamaria *et al.,* 2012). As a synthesis protocol of $Fe_3O_4/Al_2O_3/ZrO_2$ with Fe:Al:Zr mole ratios of 70:25:5 of percentage composition was prepared.

In the first step, stoechiometrically calculated $FeCl_2.4H_2O$ and $FeCl_3.6H_2O$ were accurately weighed and the calculated amounts were dissolved in 100 mL of 0.3 M HCL solution. Then, the solution was added drop wise from separatory funnel into the solution of 120 mL of 3 M NaOH over a period of 2 h, under vigorous stiring at 80^oC in N_2 atmosphere. During this process, the pH of mixture is kept at 12.0 using 0.1 M, 0.01 M and 0.001 M NaOH or HNO_3 solutions. The suspension was left undisturbed for 4 h and then the settled phase was separated from the liquor and washed with deionized water several times to obtain a suspension of Fe_3O_4 ferrofluid. The magnetite–alumina–zirconia oxide nanocomposite of each composion was prepared by adding 100 mL of $Al(NO_3)_3.9H_2O$ and $ZrOCl_2.8H_2O$ (obtained by dissolving stoichiometric amounts of both salt in 100 mL of DI- water) into the obtained Fe_3O_4 suspension and ultrasonicated for 10 min prior to use. The pH of the mixtures was adjusted to 8.0 using 0.1 M, 0.01 M and 0.001 M NaOH and HCl. Then mixture was magnetically stirred under N_2 atmosphere for 1.5 h at 70^oC.

Finally the resulting magnetic compound was separated by permanent magnet, washed with deionized water several times to remove impurities such as Cl^-, NO_3^- and excess OH^- ions and then dried at 60^oC for 24 h to obtain the desired products.

3.4.3. Elemental Analysis

The percentages of iron as iron oxide in all the as-synthesized powder were determined by flame atomic absorption spectrophotometer. 0.1 g of the as-synthesized powders were digested with concentrated nitric acid (7 mL), concentrated hydrochloric acid (4 mL) and hydrogen peroxide (2 mL) using acid digestion tube till the appearance of a clear solution. The samples were transferred to 100 mL volumetric flasks and brought to volume using deionized water. 1 mL of this solution was diluted further to 50 mL and the concentration of iron, aluminum and zirconium were read from the solution in 50 mL volumetric flasks.

3.5. Characterization of the Nanosorbent

The surface functional groups of the selected nanocomposite with maximum surface area were examined by FT-IR. The crystalline phases and the crystallite sizes were determined from its X-ray diffraction (XRD) pattern; surface area of all the adsorbents were determining by Brunauer–Emmett–Teller (BET) analysis. The concentrations of Fe and Zr metal component in the selected composite were analyzing by Flame atomic absorption spectroscopy (FAAS).

3.6. Batch Adsorption Studies

Batch mode adsorption studies for Cr(VI), Pb(II) and Cd(II) were carried out in 50 mL Erlenmeyer flask. The batch adsorption process was optimized with respect to pH, adsorbent dose, speed of agitation, contact time and initial concentration. For each run, the resulting suspension of each ion was filtered using Whatman No.41 filter paper and the filtrate was analyzed by FAAS. Removal efficiency of the adsorbent was finally determined by using the relationship given below.

$$\text{Adsorption}\% = \frac{(C_i - C_e)}{C_i} \qquad (11)$$

where C_i = the initial concentrations (mg/L) and C_e = final concentrations (mg/L) of the Cr (VI)/Pb (II) /Cd(II) ions (Amiri *et al.,* 2014).

The adsorption capacity of the Cr (VI)/Pb (II) /Cd(II) ions are the concentration of the Cr (VI)/Pb (II) /Cd(II) ion on the adsorbent mass and were calculated based on the mass balance principle,

$$Q_e = \frac{(C_i - C_e)V}{m} \quad (12)$$

where: Q_e = adsorption capacity of adsorbent (mg/g), V = the volume of reaction mixture (L), m = the mass of adsorbent used (g), C_i = the initial concentrations (mg/L) and C_e= final concentrations (mg/L) of the Cr (VI)/Pb (II) /Cd(II) ion (Amiri *et al.,* 2014).

3.6.1. Effect of Solution pH

To study the influence of pH on the present adsorption process, experiments were carried out by adding 0.1 g of the adsorbent into 50 mL Erlenmeyer flask containing 25 mL of 30 mg/L of the respective metal ions. Then the pH of the solutions was varied to 2, 3, 4, 7 and 9 before adsorption experiments were carried out while keeping other parameters constant (agitation speed at 120 rpm and contact time at 24 h. Each time the pH of the solutions was adjusted with dilute HCl and/or NaOH solutions. Then equilibrium Cr(VI), Pb(II) and Cd(II)) ions concentrations were measured after the solutions were filtered. Then the pH at which maximum adsorption was obtained was take as the optimum value for consecutive experiment(Kaewsarn *et al.,* 2008).

3.6.2. Effect of Adsorbent Dosage

The effect of adsorbent dose was determined by varying the dose as, 0.05, 0.075, 0.1, 0.5, 1 and 2 g, with initial metal ions concentration, agitation speed and contact time kept constant, and the pH value kept at the optimized values. Then the adsorbent dose at which maximum adsorption was obtained was taken as the optimum value for consecutive experiment.

3.6.3. Effect of Contact Time

The effect of contact time on metals ions adsorption, was determined by varying the contact time as, 3, 6, 12, 16, 24 and 48 h. With pH and adsorbent dose being kept at the optimized values whereas, the agitation speed and initial metal ions concentration were kept constant. Then the

contact time at which maximum adsorption was obtained was taken as the optimum value for consecutive experiment (Gupta and Nayak, 2012).

3.6.4. Effect of Agitation Speed

To study the effect of agitation speed on Cr(VI), Pb(II) and Cd(II) ion adsorption, the agitation speed varied as, 50, 100, 120, 140, 160 and 200 rpm with pH, adsorbent dose and contact time kept at optimized value, whereas initial metal ions concentration was kept constant. the quantity of Cr(VI), Pb (II)and Cd(II) ions adsorbed was determined. Then the agitation speed at which maximum adsorption was obtained was taken as the optimum value for consecutive experiment (Hadjmohammadi *et al.,* 2011).

3.6.5. Effect of Initial Concentration

To study the effect of initial adsorbate concentration, the experiment was carried out at different initial (Cr(VI), Pb (II) and Cd(II)) ions concentrations (10, 20, 30, 50, 100, 150 and 200 mg/L). With pH, adsorbent dose, contact time and agitation speed kept at optimized values. Then the initial adsorbate concentration at which maximum adsorption was obtained was taken as the optimum value for consecutive experiment (Khazae *et al.,* 2011).

3.7. Effect of Interfering Ions

The effects of coexisting cations such as K^+, Ca^{2+}, Mg^{2+} and Fe^{3+} on Pb(II), Cd(II) and Cr(VI) adsorption by the synthesized adsorbents were investigated by performing Pb(II), Cd(II) and Cr(VI) adsorption under fixed optimized conditions. The dependency of Pb(II), Cd(II) and Cr(VI) ions adsorption on the as synthesized powder in the presences of a series of concentrations of each target cations, K^+, Ca^{2+}, Mg^{2+} and Fe^{3+} (20 mg/L for each, respectively) at optimized initial Pb(II) (20ppm), Cd(II) (20ppm) and Cr(VI) (20ppm) concentration was investigated. Both the effect of mixture of cations and the effect of individual cations were studied to estimate the selectivity of the adsorption for Pb(II), Cd(II) and Cr(VI) ions.

3.8. Point of Zero Charge Determination

The determination of Point of Zero Charge (pzc) of the as-synthesized Fe-Al-Zr adsorbent assessed. To this effect 50 mL of 0.001M $NaNO_3$ solution was added to 0.1 g of Fe-Al-Zr ternary mixed oxide nanocomposite and adjusted to various pH values ranging from 2-12 by using dilute HNO_3 or NaOH solutions in a 250 mL beaker. After equilibrating the mixed solution for 60 min in a mechanical shaker the initial pH was determined. Then 1 g of $NaNO_3$ was added to the above and further equilibrated for another 60 min and the final pH was measured. The graph of $pH_{final-initial}$ (Y-axis) versus pH_{final} (X-axis) was plotted from which the point of zero charge was determined as the point where the graph intersects the X-axis (Panumati *et al.,* 2008).

3.9. Adsorption Isotherms

The adsorption isotherms were used to characterize the interaction of each analyte ions with adsorbent. Equilibrium data are usually described by various adsorption isotherms. Two isotherm equations were used in the present study, Langmuir and Freundlich. (Netzer and Wilkinson, 1974).

The Langmuir equation is:

$$C_e/q_e = 1/(b\ q_{max}) + (C_e / q_{max}) \quad (13)$$

The Freundlich equation is:

$$\text{Log } q_e = \text{Log } K_f + (1/n) \text{ Log } C_e \quad (14)$$

Where q_e is the amount of adsorbed material at equilibrium (mg/g), C_e is the equilibrium metal ions concentration of the adsorbate (mg/L), q_{max} (mg/g) and b (L/mg) are the Langmuir constants, and K_f and n are Freundlich constants.

3.10. Adsorption Kinetics

The adsorption kinetics of Pb(II) ,Cr(VI) and Cd(II) ions was determined by varying the contact time as, 3, 6, 12, 16, 24 and 48 h by keeping all parameters (pH, adsorbent dose, contact time,

agitation speed and initial concentration) at optimized values. It was evaluated by using optimized dose of adsorbent and placed in several 50 mL Erlenmeyer flasks, each containing 25 mL of 30 mg/L Pb(II), Cr(VI) and Cd(II) ions solution. The pH of the solution was maintained at the optimized value. The flasks were stoppered and continuously shaked at a speed of 100 rpm. The sample solution was immediately filtered and then quilibrium concentration was analyzed. For all the above parameters, percent of adsorption (%) was calculated using the following equation: (Gupta and Nayak, 2012).

$$\text{Percent of adsorption (\%)} = \frac{C_o - C_e}{C_o} * 100 \quad (15)$$

3.11. Thermodynamic Study

In order to determine the effect of temperature on sorption phenomenon, all predetermined and optimized values of the parameters (pH, dosage, contact time, speed of agitation and concentration) were used and the temperature was established at 30, 40, 50 and 60^{o}C.The thermodynamic parameters such as change in standard free energy (ΔG), enthalpy (ΔH) and entropy (ΔS) can be calculated by using the following equation: (Buzuayehu, 2012).

$$\Delta G = -nRT\ln K_c \quad (16)$$

$$\Delta G = \Delta H – T\Delta S \quad (17)$$

$$\ln K_c = \Delta S/R - \Delta H/RT \text{ ,where } \ln K_c = q_e/C_e \quad (18)$$

Where R (8.314 J/molK) is the gas constant, T (K) is the absolute temperature and K_c (cm^3g^{-1}) is the standard thermodynamic equilibrium constant defined by q_e/C_e. By plotting the graph of $\ln K_c$ versus T^{-1}, the value of ΔH and ΔS can be estimated from the slopes and intercept. Thermodynamic considerations of an adsorption process are necessary to conclude whether the process is spontaneous or not. Gibb's free energy change, Δ*G*, is the fundamental criterion of spontaneity. Reactions occur spontaneously at a given temperature if Δ*G* has a negative value.

3.12. Desorption Study

The powder was immersed in the regenerating solution and placed in a shaker at 25^{o}C for 12 h. To this, 0.1 M NaOH solution was addded for desorption to take effect. The desorbed adsorbate in the solution was finally recovered by filtration and analyzed for the corresponding metal ion concentration. The recovery percentage was obtained from the following relation.

$$\text{Desorption Efficiency } \% = \frac{Desorbed}{adsorbed} \times 100 \quad (19)$$

Where,

Desorbed =the concentration and/or the mass of the metal ion after the desorption process

Adsorbed =($C_o - C_e$) for each recovery process.

3.13. Recyclability Study

To investigate the extent of regeneration and reusability of the adsorbent, metal ion solutions of constant feed concentration (20 mg L^{-1}) was run through the optimum dose (0.1, 0.5, 1 mg) of the adsorbent for 6 and 4 h. After the completion of each run, the adsorbent were washed thoroughly with 0.1 M NaOH solutions, for 15 min in continuous recycle modes. Desorption of metal ion by 0.1 M NaOH solution was reported. Next, the systems were washed with distilled water for thirty minutes, until the permeate would have the same pH as cleaning water. After washing, permeability value was checked (Raka and Sirshendu, 2014).

3.14. Effect of Ionic Strength

The effect of ionic strength (0.02 to 0.1 M $NaNO_3$) on the adsorption capacity of Fe-Al-Zr in the removal of Cd(II), Cr(VI) and Pb(II) was investigated. About 1 g, 0.1 g and 0.5 g of Fe-Al-Zr were placed in a 125 mL Erlenmeyer flask at an initial concentration of 20 mg L^{-1} and initial pH of 6, 4 and 6. The samples were agitated using a shaker bath at 120 rpm and 100 rpm for 12 h and 6 h respectively (Franus and Bandura, 2014).

4. RESULTS AND DISCUSSION

4.1. Characterization of as-synthesized Adsorbent

4.1.1. XRD Patterns

X-ray diffraction (XRD) is one of the most important non-destructive tools to analyze all kinds of matter-ranging from fluids, to powders and crystals. From research to production and engineering, it is an indispensable method for materials characterization and quality control (Yohannes, 2014). The XRD patterns of the Fe-Al-Zr ternary oxide nanocomposite before (Figure A) and after (Figure B) adsorption experiments were demonstrated in Figure 1. It was observed that very weak intensities on a broad background suggesting the amorphous nature of the composite. However, the presence of some sharp intensity peaks at 2θ values 35.25, 43.32, 43.42, 53.69 and 63.33° indicates the formation of some crystal at very small scale up on formation of nanocomposite structure (Bamlaku *et al.,* 2016).

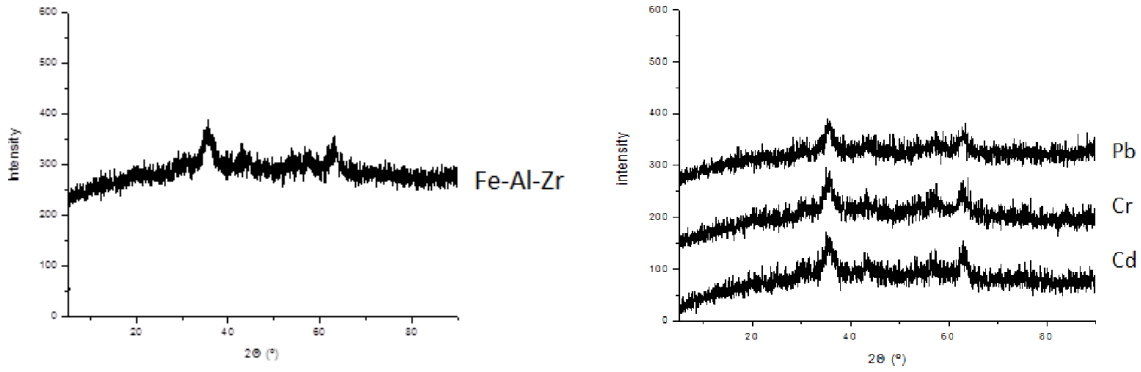

A B

Figure 1. (A) XRD pattern of before adsorption of Fe-Al-Zr, (B) XRD pattern after adsorption for Pb(II), Cr(VI) and Cd(II)of Fe-Al-Zr.

As observe XRD pattern of before (Figure A) adsorption and pattern of after (Figure B) adsorptions of Fe-Al-Zr nanocomposite there are no different between them possible.

4.1.2. Brunauer–Emmett–Teller (BET) Surface Area

Surface area of the Fe-Al-Zr nanocomposite was determined by the Brunauer–Emmett–Teller (BET) method (acquisition and reduction). Using N_2 adsorption technology, the surface areas of the prepared magnetic nanocomposite was determined. According to literature, the composition of Fe-Al-Zr nanocomposite had an obvious impact on the surface areas (BET). There was an appreciable variation in BET with the increase of ZrO_2–Al_2O_3 contents. On the other hand, addition of alumina component to the catalysts resulted in an increased trend of the surface areas (Anqi *et al.,* 2014).

The BET (surface area) of the Al-Fe-Zr ternary oxides nanocomposites with 25:70:05 mole ratios was measured. The measured surface areas of 25:70:05 of the Al:Fe:Zr mole ratios was found to be 205 m^2/g. The result showed that the sample has relatively large surface area.

Previews work (fekadu, 2015) of at the same mole ratio and nanocomposite but the surface area with this work is higher which mean that 295 m^2/g>205 m^2/g. The differences between them are only technical of washed for several time possibly.

4.1.3. Infrared Spectroscopic Studies

The FT-IR spectra of ternary nanocomposite display a number of peaks before and after Pb(II), Cd(II) and Cr(VI) adsorption (Fig. 2). The peaks observed in both cases are more or less similar. The absorption bands observed from (3500–3000 cm^{-1}) centered at 3424 cm^{-1}, 3414 cm^{-1} and 3412 cm^{-1} represent O-H stretching vibrations of adsorbed water molecules. The absorption bands observed at 1626-1628 and 1375 cm^{-1}could be attributed to H-O-H bending vibration and Al-O stretching, respectively and the strong Fe–O absorption bands around 583.5-591.48 cm^{-1} corroborates that the main phase of as-prepared particles is magnetite. Another important adsorption band can be observed at 441.45 cm^{-1}, which corresponds to the vibration of the Zr-O bond in the Fe-Al-Zr powders (Julio *et al.,* 2012).

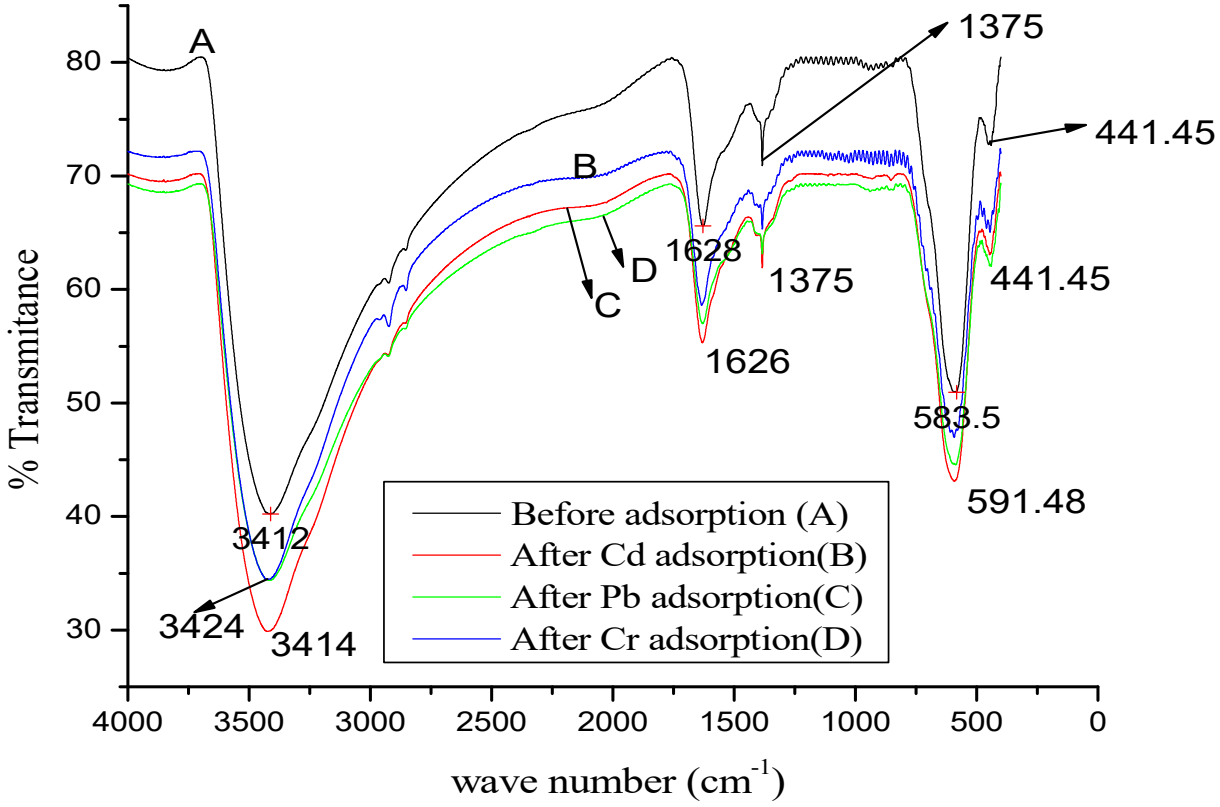

Figure 2. FT-IR spectra of Fe_3O_4/ Al_2O_3/ZrO_2 before (A) and after (B, C and D), respectively.

From the FTIR spectra, it could be concluded that specific adsorption of aqueous metal ions occurred on the Fe–Al–Zr ternary nanocomposite sorbent in consequence of the exchange of surface hydroxyl groups by metal ions, assuming this is to be the main adsorption mechanism.

4.1.4. Elemental Analysis of the Adsorbent

The FAAS results indicated that the percentage compositions of Fe, Al and Zr in the as synthesized selected nanocomposite were found to be 72.3, 23.9 and 3.8%, respectively, but the expected values of the oxides are 70% for iron, 25% for aluminum and 5% for zirconium and this is not far from the theoretical compositions of the metals: Fe, Al and Zr, respectively. The

difference in the percentage compositions of iron, aluminum and zirconium (between actual and theoretical values) may be due to insufficient dissolution, vaporization and lack of atomization.

4.1.5. Point of Zero Charge Determination

The point of zero charge of the adsorbent Fe-Al-Zr was determined from the graph of pH (final-initial) vs pH(final) for 0.1 mg of the adsorbent. The point of zero charge is the point at which the surface acidic or basic functional groups no longer contribute to the pH value of the solution. The pH_{PZC} of an adsorbent is a very important characteristic that indicates the pH at which the adsorbent is neutral, whereas below and above this pH, the adsorbent becomes either positively or negatively charged (Abia or Asuquo, 2008).

The pH_{PZC} of Fe-Al-Zr nanocomposite sorbent was found to be around 5.71 as shown in Figure 3. Therefore, the surface of the adsorbent being charged negatively at pH greater than 5.71 and any anion should be repelled from the surface, whereas the surface of the adsorbent was charged positively at pH lower than 5.71 and electrostatic attraction could occur between the surface and the anion, favoring the accumulation of the Cr (VI) anion on the surface of adsorbent (Paola *et al.,* 2006).

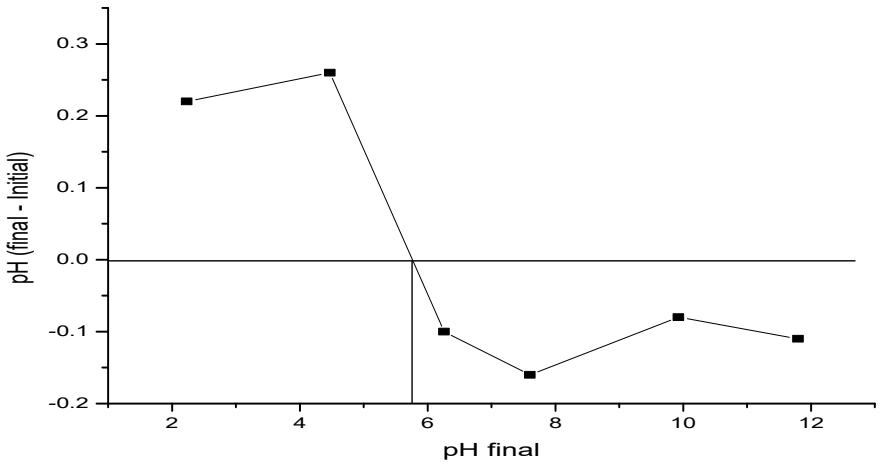

Figure 3. pH point zero charge (pHpzc) for $Fe_3O_4/Al_2O_3/ ZrO_2$

4.2. Optimum Conditions

4.2.1. Effect of pH

pH is one of the most important factors that influences most adsorption process. The effect of pH on the extent of adsorption of Pb(II), Cd(II) and Cr(VI) ions onto the nanocomposite adsorbent was investigated by varying the pH range from 2 to 9 and keeping other parameters constant at: metal ion concentration of 30 mg/L, adsorbent dose of 0.1 g, agitation speed of 120 rpm and contact time of 24hrs. As the result shows (figure 4) Pb(II), Cd(II) and Cr(VI) ion removal was low at pH low, due to the fact that the higher concentration and mobility of hydrogen ions (H^+) present at lower pH favored the preferential adsorption of hydrogen ions than metal ions. After reached a maximum efficiencies at pH 6, and adsorption decreased slowly from pH 6 to 9, while for Cr(VI) that was maximum efficiency at pH 2–4 and decreased slowly from pH 4 to 9. The Fe-Al-Zr displayed a maximum Pb(II), Cd(II) and Cr(VI) removal efficiencies of 97.76%, 99.88% and 96.3% at pH 6 and 4 respectively. Therefore, pH 6 appeared to be the optimal condition, and it was chosen as the optimal pH and slightly diminished after pH 6. This might be due to the weakening of electrostatic force of attraction between the oppositely charged adsorbate and precipitation of $Pb(OH)_2$ and $Cd(OH)_2$ and the (CrO_4^{2-}) at higher pH values with lead, cadmium and chromium ions (Anbiaa *et al.,* 2015) for active site of nanocomposite adsorbent led to decrease the removal efficiency of Pb(II), Cd(II) and Cr(VI) ions using Fe-Al-Zr ternary nanocomposite. The reason for the out-standing adsorption capacity of Cr(VI) over Fe-Al- Zr observed at low pH may be attributed to that the large number of H^+ presented at these pH, which protonated on the surface of Fe-Al- Zr trenary nanocomposite. At the same time, Cr(VI) mainly exist in the form of $HCrO_4^-$,$Cr_2O_7^{2-}$and $Cr_2O_4^{2-}$in aqueous solution. The adsorption process then proceeds due to the electrostatic attraction between these two oppositely charged ions (Xiaoyao *et al.,* 2014). After optimum pH 4 adsorption efficiency of Cr(VI) decrease due to the negative charge on the Fe-Al-Zr ternary nanocomposite surface and weakening the electrostatic force between the nanocomposite and anionic Cr(VI) ions, resulting in the reduction in the adsorption rate (Barakat *et al.,* 2016).

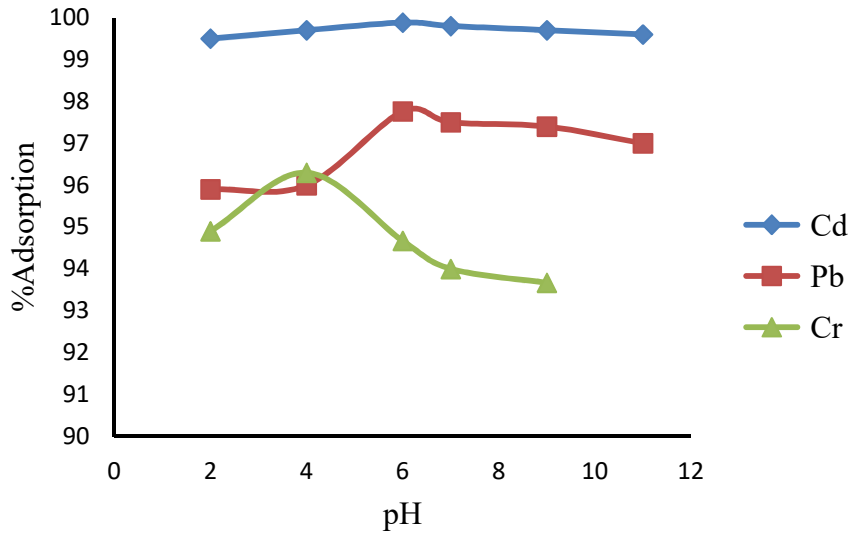

Figure 4. Effect of pH on the removal Pb, Cd and Cr at initial concentration ions (Co = 30 mg/L dose = 0.1 g, agitation speed = 120 rpm and contact time = 24 h).

4.2.2. Effect of Adsorbent Dose

The effect of adsorbent dose on the Pb(II), Cd(II) and Cr(VI) ions removal efficiency was studied by varying mass of the adsorbent ranging from 0.05 - 2.00 g and keeping other parameters constant at: pH 6 and 4, Pb(II), Cd(II) and Cr(VI) ions concentration 30 mg/l, agitation speed of 120 rpm and contact time of 24 hrs. The result in Fig. 5 shows that the adsorption efficiency increased with the adsorbent dose till 0.5 g/L for (Pb), 1 g/L for Cd (II)) and 0.1 g/L for Cr (VI). The increase in the removal efficiency may be attributed to the fact that, with an increase in the adsorbent dosage and a greater surface area or more adsorption sites for the metal ions. This figure 5 shows that the adsorption percentage becomes decrease after 0.1g for Cr(VI), 0.5 g for Pb(II) and 1 g for Cd(II) due to overlapping of adsorption sites as a result of overcrowding of adsorbent particles. At the low adsorbent dose, all types of sites are entirely exposed and the adsorption on the surface is saturated faster showing a higher adsorption capacity (qe). But, at higher adsorbent dose, the availability of high energy sites decreases with a large fraction of the lower energy sites is being occupied, resulting in a lower adsorption capacity (Hadjmohammadi *et al.*, 2011).

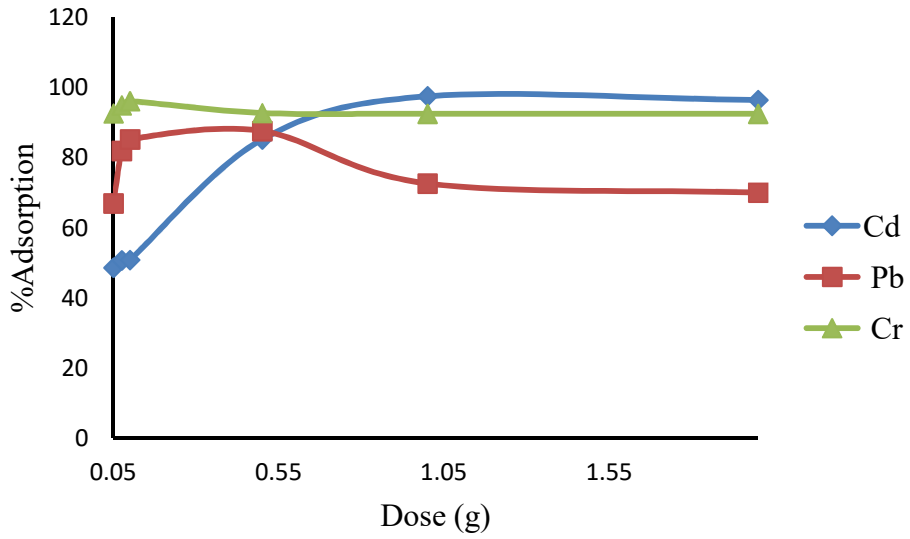

Figure 5. Effect of adsorbent dose on the removal of Pb(II), Cd(II) and Cr(VI) ions at initial Pb(II), Cd(II) and Cr(VI) ion concentration of 30 mg/L, agitation speed 120 rpm contact time 24 h and pH at optimized.

4.2.3. Effect of Contact Time

The effect of contact time on the Cd(II), Pb(II) and Cr(VI) adsorption efficiency of was studied by varying contact time from 3 to 48 h keeping other parameters constant. The optimum time for removal of Cd(II), Cr(VI) and Pb(II)was 12 and 6 h, respectively. Fig. 6 shows rapid adsorption in the initial hour from 3- 12 h for Cr(VI), 3-6 h for Cd(II) and 3- 6 h for Pb(II). That is probably due to the larger surface area of the Fe-Al-Zr ternary sorbent being available at beginning for the adsorption rate of metals. Maximum removal efficiency of Cd(II), Pb(II) and Cr(VI) was attained by the trenary nanocomposite 98.8%, 94.4% and 94.6%, respectively within 12 h, and 6 h of contact time; in all cases equilibrium was achieved within these respective length of time. The figure 6 show that in all case the rate of the percentage of heavy metal ions removal is decease for further increase time due to the surface adsorption sites become exhausted, the uptake rate is controlled by the rate at which the adsorbate. This result is interesting because equilibrium time is one of the important considerations for economical wastewater treatment applications. Maximum Cr(VI) and Cd(II) removal was achieved within 12 h after which Cr(VI) and Cd(II) concentration in the test solution became constant. It may be explained by the fact that initially for adsorption large number of vacant sites was available, which slowed down later due to

exhaustion of available surface sites and repulsive force between solute molecules and the bulk phase (Amiri *et al.,* 2014).

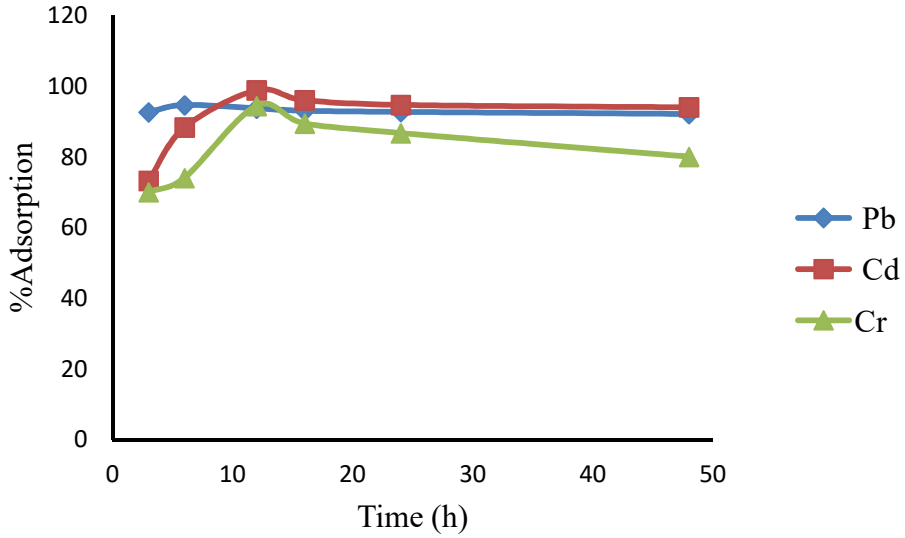

Figure 6. Effect of contact time optimization on the removal of Cd (II), Pb (II) and Cr (VI) ions (Co = 30 mg/L, pH = 6 and 4 in Fe-Al- Zr; adsorbent dose = 1 g (Cd (II)), 0.1 g Cr (VI) and 0.5 g Pb (II); agitation speed = 120 rpm.

4.2.4. Effect of Agitation Speed

Effect of agitation speed on adsorption of Cd(II), Pb(II) and Cr(VI) was investigated Fig.7, at initial Cd(II), Pb(II) and Cr(VI) ions concentration of 30 mg/L and pH (6 and 4) and varying the agitation speed from 50 to 200 rpm. It can be easily observed in Fig.7, that the adsorption efficiency of Fe-Al-Zr ternary nanocoposite adsorbent increases initially as the agitation speed increased from 50 to 120 rpm for Cd(II) and Cr(VI) (69% to 93.4% and 72% to 81.5%, respectively) and Pb(II) from 50 to 100 rpm (84.4% to 90.9%). This result can be associated with the fact that the increase in the agitation speed could improve the diffusion of solute toward the adsorbent surface. This is because with low agitation speed the greater contact time is required to attend the equilibrium. With increasing the agitation speed, the rate of diffusion of Cd(II), Pb(II) and Cr(VI) ions from bulk liquid to the liquid boundary layer surrounding the particle become higher because of an enhancement of turbulence and a decrease of thickness of the liquid boundary layer (Satish, *et al*., 2011). But, beyond to optimum of 100 rpm for Pb(II), 120 rpm for Cd (II) and Cr(VI) this agitation speed the adsorption efficiency decreased because of more

agitation speed causes more desorption of Pb (II), Cd(II) and Cr(VI) ions from the adsorption site.

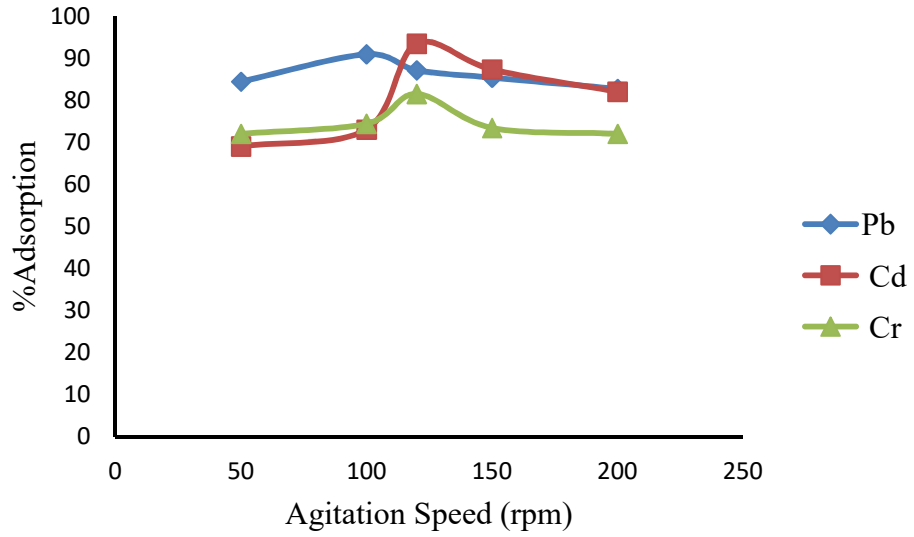

Figure 7. Effect of speed of agitation on the removal of Cd (II), Pb (II) and Cr (VI) ions (At Co = 30 mg/L, pH = 6 and 4 respectively, adsorbent dose = 1 g, 0.5 g and 0.1 g and at optimized contact time)

4.2.5. Effect of Initial Concentration

The sorption of Cd(II), Cr(VI) and Pb(II) on Fe-Al-Zr nanocomposite was studied as a function of initial Cd(II), Cr(VI) and Pb(II) ions concentration. Figure 8 shows the removal efficiency of Pb(II), Cr(VI) and Cd(II) metal ions with its concentration. It is observed that the removal efficiency of Pb(II), Cr(VI) and Cd(II) metal ions is high at lower concentration and gradually decreases as the concentration of metal ions increase. The removal efficiency of the Cd(II), Cr(VI) and Pb(II) ions decreased from 96.65% at 20 mg/L to 87.3% at 200 mg/L for Cd(II), from 96.55% at 20 mg/L to 85.2% at 200 mg/L for Cr(VI) and 97.20% at 20 mg/L to 70.80% at200 mg/L for Pb(II). This can be explained by the fact that in case of low concentrations, the ratio of the initial number of moles of solutes to the available surface area of adsorbent is large and subsequently the fractional adsorption becomes independent of initial concentration and consequently higher adsorption yields were obtained. However, at higher concentrations, most of the adsorption sites could be occupied by ions and the available sites of adsorption would

become fewer, hence the percentage removal of metal ions which depends up on the initial concentration could decrease (Yu et al., 1990).

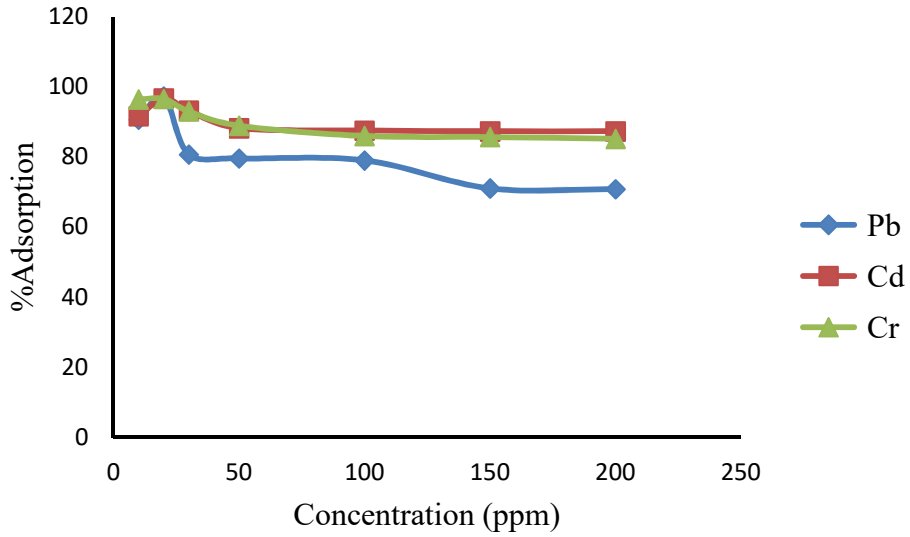

Figure 8. Effect of initial concentration of Cd (II), Cr (VI) and Pb(II) ions on the removal of Cd (II), Cr(VI) and Pb(II) ions, pH at 6, 4 and 6, adsorbent dose = 1, 0.1 and 0.5 g, agitation speed = 120 and 100 rpm and at optimized contact time).

4.2. Adsorption Isotherm

Adsorption isotherms are the basic requirements for designing any sorption system. The adsorption isotherms show the relationship between initial metal ion concentrations in solution and the amount of metal ions adsorbed on a specific sorbent at a constant temperature, leading to find the best equilibrium position in the adsorption process. Various isotherm models can be used to analyze adsorption data. The most common ones are the Langmuir and the Freundlich models.

The Langmuir isotherm model describes the adsorption of an adsorbent on a homogeneous, smooth surface of an adsorbent, and each adsorptive site can be occupied only once in a one on one manner. The empirical Freundlich model is based on the sorption on reversible heterogeneous surfaces (Zare *et al.,* 2014).

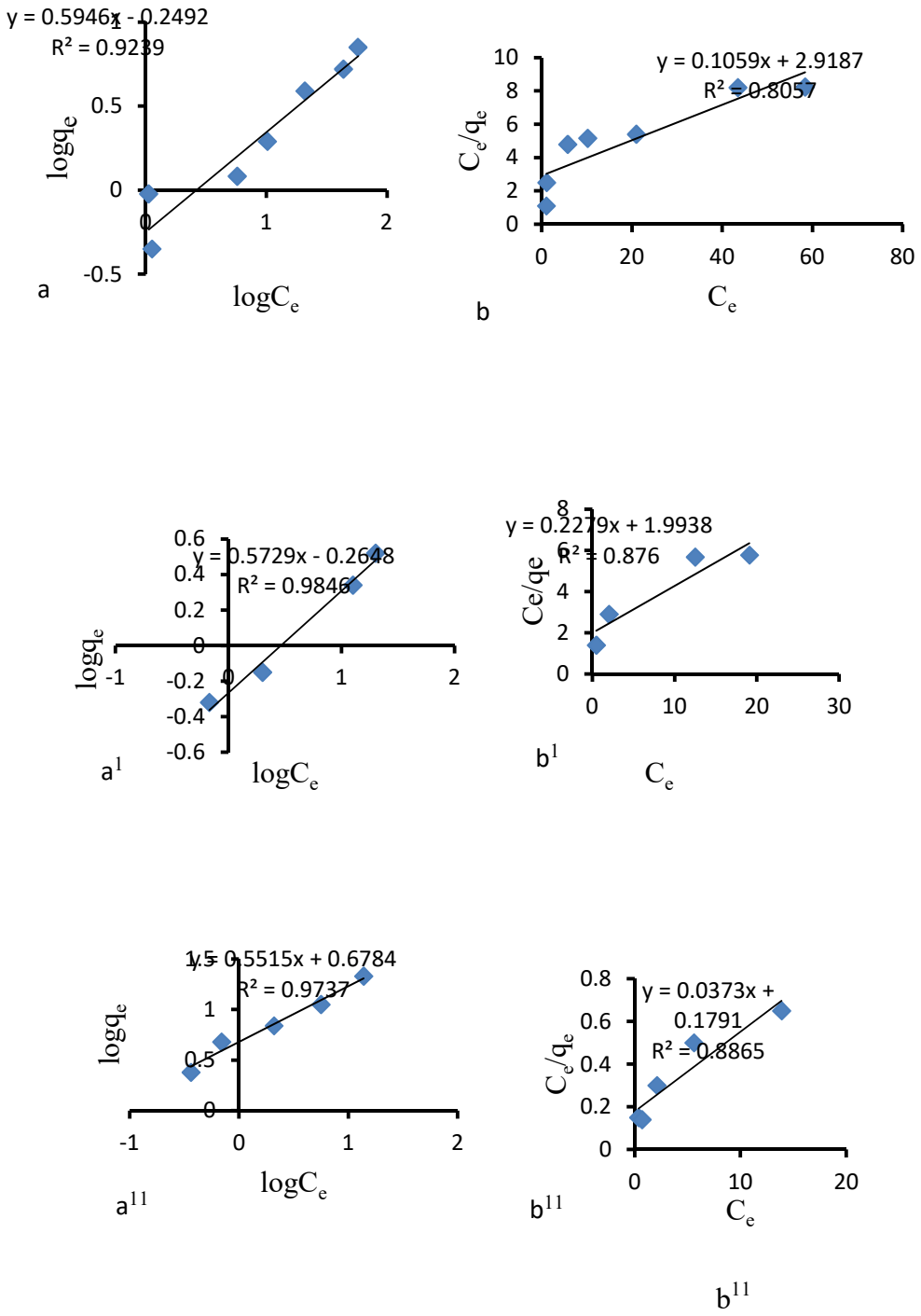

Figure 9. Freundlich (a, a^1, a^{11}) and Langmuir (b, b^1, b^{11}) adsorption isotherm of Cd (II), Cr (VI) and Pb(II)ions by Fe-Al-Zr ternary mixed oxide.

The linearized Langmuir (Langmuir, 1918) and Freundlich (Freundlich, 1906) plots are given in Figure 9 (a, a^1, a^{11}) and 9 (b, b^1, b^{11}), respectively. The slopes and intercept of the linearized

Freundlich and Langmuir plots were used to calculate the adsorption constants tabulated in Table 1. From Table 1, the higher coefficients of determination isotherm indicates that the Freundlich model fits the adsorption data better than Langmuir model.

As can be seen from Figure 9 (b to b[11]), the plot of Ce/qe vs Ce yields a straight line with a slope, intercept, Q_{max} and b value of 0.1059, 2.9187, 9.44 and 0.036 respectively for Pb (II) ion; Similarly the slope, intercept, Q_{max} and b values of 0.2279, 1.9938, 4.38 and 0.11 have been disturbuted for Cd (II) ion and 0.0373, 0.1791, 26.8, and 0.21, respectively, for Cr(VI) ion.

For Langmuir isotherm the essential characteristics can be expressed in terms of a dimensionless equilibrium parameter (R_L). The value of R_L indicates the type of the isotherm to be unfavorable ($R_L>1$), linear($R_L=1$) or favorable($0<R_L<1$). As it can be seen from the appendix table 9, R_L value for all concentration is in between 0 and 1 indicating a favorable adsorption.

From the plot of log q_e vs log C_e, Figure 9 (a - a[11]) yields a straight line with a slope 0.5946 and an intercept 0.2492 for Pb(II) ion, slope 0.5729 and intercept 0.2648 for Cd(II) ion and also slope 0.5515 and the intercept 0.6784 for Cr(VI) ion. The n value indicates the degree of nonlinearity between solution concentration and adsorption as follows: if $n = 1$, then adsorption is linear; if $n < 1$, then adsorption is a chemical process; if $n > 1$, then adsorption is a physical process. The n value in Freundlich equation was found to be1.74, 1.80 and 1.67 for Cd (II), Cr(VI) and Pb(II) ions, respectively (Table 1). The situation $n > 1$ is most common and may be due to a distribution of surface sites or any factor that causes a decrease in adsorbent adsorbate interaction with increasing surface density and the values of n within the range of 1–10 represent good adsorption (Mulu Berhe, 2013). In the present study, since n lies between 1 and 10 it indicates the physical adsorption of metal ions onto Fe-Al-Zr.

Langmuir and Freundlich adsorption constants and coefficients of determination (R^2) are presented in Table 1. To find the most appropriate model for the metal ions adsorption; data were fitted to Freundlich isotherm models. Results revealed that Freundlich adsorption isotherm was the best model for the metal ions adsorption onto Fe-Al-Zr with R^2 of 0.9846, 0.9737 and 0.9239 for Cd(II), Cr(VI) and Pb(II), respectively.

Table 1 Langmuir and Freundlich isotherm constants for Cd(II), Cr(VI) and Pb(II) ions adsorption by Fe-Al-Zr ternary mixed oxide.

Adsorbant	Langmuir isotherm model				Freundlich isotherm model		
	Q_{max}	b	R_L	R^2	K_f	n	R^2
Cd	4.38	0.11	0.3	0.876	0.54	1.74	0.9846
Cr	26.8	0.21	0.19	0.8865	4.77	1.80	0.9737
Pb	9.44	0.036	0.58	0.8057	0.56	1.67	0.9239

4.3. Kinetics of Adsorption

The adsorption kinetics is quite important in wastewater treatment because it controls the solute removal rate, which in turn controls the residence time of solute uptake at the solid–liquid interface. Actually, adsorption kinetics is one of the most imperative characteristics that signifies the adsorption efficiency. The adsorption kinetics process was investigated by various kinetic models such as pseudo–first–order and pseudo–second order equations.

The Lagergren pseudo–first-order kinetic model is the most popular kinetic equation based on the assumption that the adsorption rate is related to the number of unoccupied adsorptive sites and used only for the rapid initial phase. On the other hand, the adsorption rate could also be approximated by the pseudo–second-order kinetic model. This model is more likely to predict the kinetic behavior of adsorption with chemical sorption being the rate-controlling step (Zare *et al.,* 2014).

The kinetics of Cd(II), Cr(VI) and Pb(II) adsorption on the Fe-Al-Zr ternary nanocomposite were analyzed using pseudo first-order and pseudo second-order kinetics models (Figures 10). The conformity between experimental data and the model predicted values was expressed by the coefficient of determination (R^2, values close or equal to 1). As seen in Table-2, the value of R^2 calculated from pseudo-second order kinetics is almost higher. These results indicate that the adsorption of Cd(II), Cr(VI) and Pb(II) on the Fe-Al-Zr ternary nanocomposite sorbent follows pseudo-second order kinetics. The values of rate constant (k) and coefficient determination (R^2) are as reported in Table-2 for the two models.

The kinetic curves obtained for the adsorption of Cd(II), Cr(VI) and Pb(II) ions from aqueous solutions onto the Fe-Al-Zr ternary nanocomposite sorbent are shown in figure 1

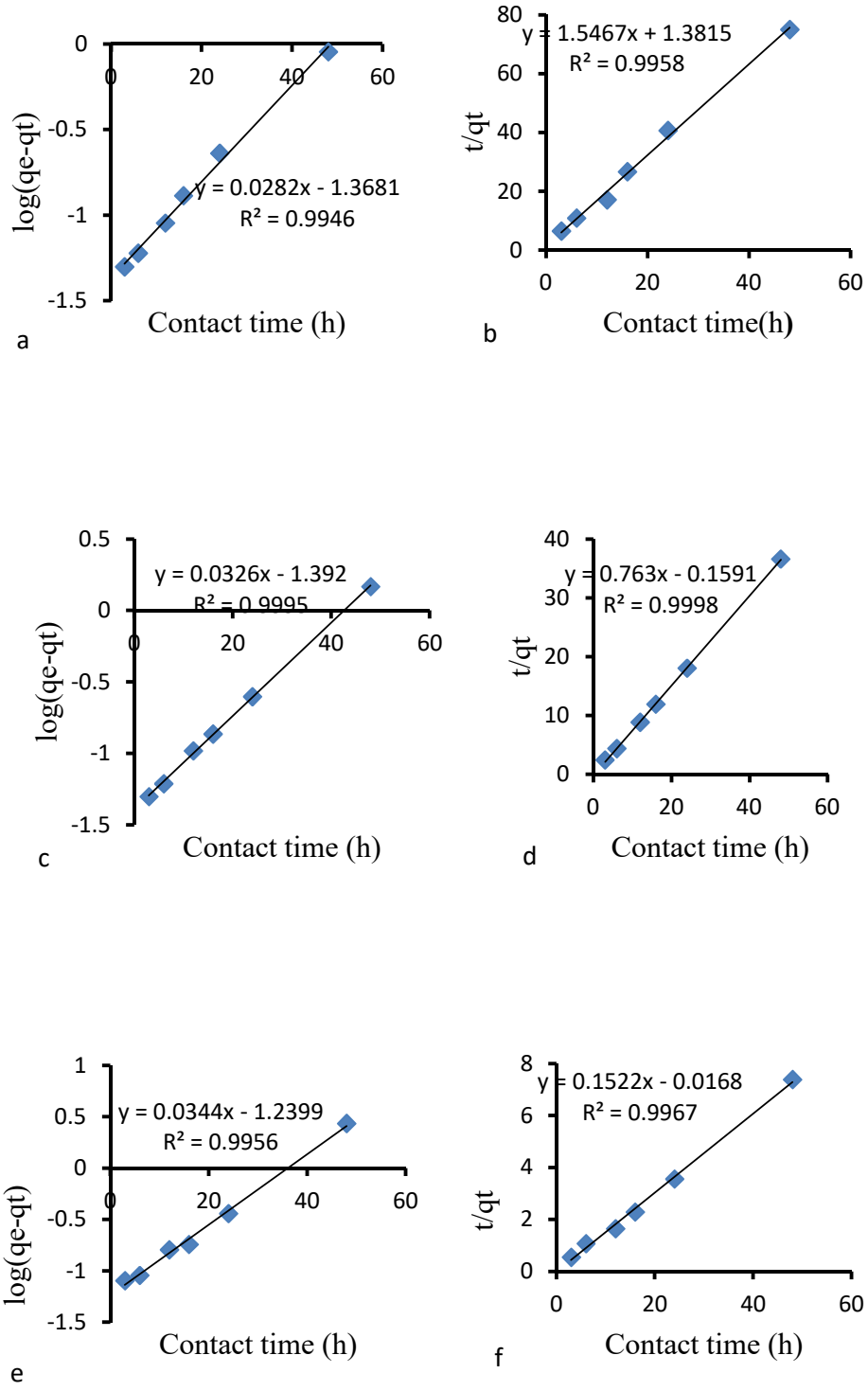

Figure 10. Plot of the pseudo-first order (a, c, and e) and pseudo-second order (b, d and f) onto Al-Fe-Zr nano sorbent respectively.

From the slopes and intercepts of Pseudo-first order model [log (q_e-q_t) vs t] figure 10 (a, c and e), the first order rate constant k_1 and equilibrium adsorption density q_e were determined. And from the slopes and intercepts of Pseudo-second order model, t/q_t vs t (figure 10 b, d and f), the values of k_2 and q_e were determined. The kinetic parameters obtained from the models are given in table 2.

Pseudo second-order reaction rate model which give a linear relationship adequately described the kinetics of sorption of Cd(II), Cr(VI) and Pb(II) ions with high coefficient of determination (R^2 = 0.9958, 0.9967 and 0.9998) in Fe-Al- Zr nanocomposite sorbent respectively. This study indicated that the pseudo-second order model better represents the Cd(II), Cr(VI) and Pb(II) ions adsorption kinetics.

Table 2. The values of parameters and correlation coefficients of kinetic models.

	Cd			Cr			Pb		
	k	q_e (mg/g)	R^2	k	q_e (mg/g)	R^2	k	q_e (mg/g)	R^2
Pseudo first order	0.065	0.043	0.9946	0.079	0.0575	0.9956	0.075	0.04	0.9995
Pseudo second order	1.73	0.646	0.9958	1.37	6.57	0.9967	3.7	1.3	0.9998

4.4. Thermodynamics of Adsorption

The thermodynamic parameters such as change in standard free energy (ΔG), enthalpy (ΔH) and entropy (ΔS) can be calculated by using the following equation:

$$\Delta G = -RT \ln Kc \quad (20)$$

$$\ln Kc = \frac{\Delta S}{R} - \frac{\Delta H}{RT} \quad (21)$$

Where R (8.314J/mol K) is the gas constant, T(K) is the absolute temperature and Kc is the standard thermodynamic equilibrium constant defined by qe/Ce. By plotting the graph of lnKc versus T^{-1}, the value of ΔH and ΔS can be estimated from the slopes and intercept. The result of ΔG^0, ΔH^0 and ΔS^0 are shown in Fig.11. All the thermodynamic parameters are listed in Table 3.

The negative values of Gibbs free energy for all the metal ions demonstrated that the adsorption process was spontaneous. Furthermore, it was also verified by the fact that the enthalpy values of the adsorption (ΔH^0) were positive, characterizing the process as endothermic (wang *et al.,* 2014). Additionally the positive entropy (ΔS^0) observed for all the metal ions indicated the increased randomness at the solid–liquid interface during the adsorption of Cd(II), Cr(VI) and Pb(II) (Yanga *et al.,* 2014) and the affinity of the adsorbents for Cd(II), Cr(VI) and Pb(II) ions (Zhao *et al.,* 2011).

Table 3 Thermodynamic parameters for Pb(II), Cd (II) and Cr (VI) ions adsorption onto $Al_2O_3/Fe_3O_4/ZrO_2$ adsorbent.

Types of adsorbates	T(k)	ΔG (KJ/mol)	ΔH (KJ/mol)	ΔS (J/molk)
Cd	303	-129.5	+365.8	+2.3
	313	-132.3		
	323	-135.1		
	333	-137.9		
Cr	303	-3444.96	+13052.98	+51.45
	313	-3506.8		
	323	-3568.7		
	333	-3630.6		
Pb	303	-383.9	+1330.24	+6.144
	313	-391.3		
	323	-398.7		
	333	-406.1		

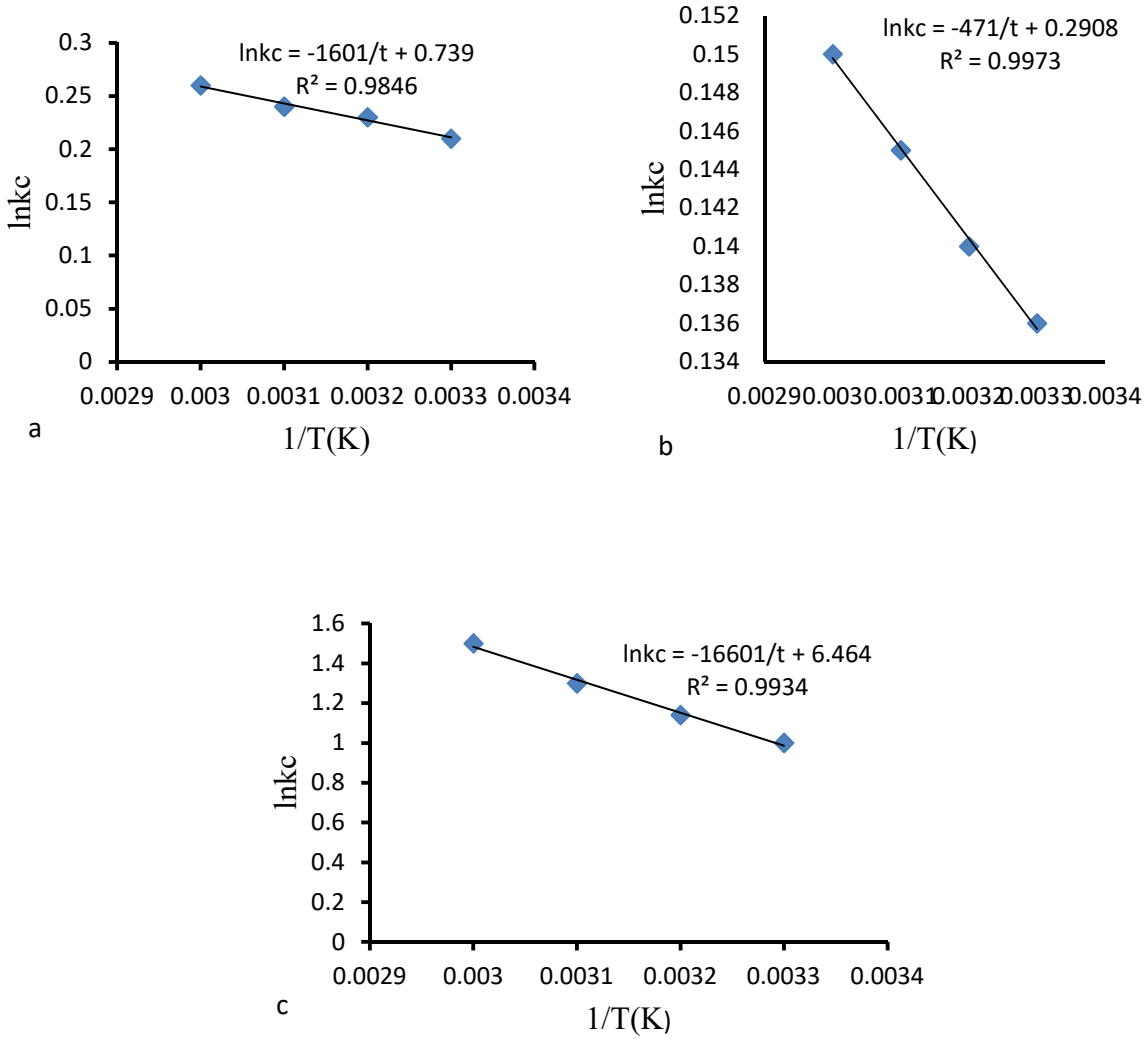

Figure 11. Plot of lnKc vs T^{-1} for Pb(II), Cd (II) and Cr (VI) ions adsorption in $Al_2O_3/Fe_3O_4/ZrO_2$ sorbents (a), at pH = 6, dose = 0.5 g, agitation speed = 100 rpm, Contact time = 6 h, Co = 20 mg/L for Pb(II), (b) pH = 6, dose = 1 g, agitation speed = 120 rpm, Contact time = 12 h, Co = 20 mg/L for Cd(II), (c) at pH = 4, dose = 0.1 g, agitation speed = 120 rpm, Contact time = 12 h, Co = 20 mg/L for Cr(VI) and respectively.

4.5. Effect of ionic Strength

Ionic strength is an important parameter especially when solute removal is affected by slight changes in the supporting electrolyte solution. The concentration of $NaNO_3$ was varied from 0.00 to 0.1 M, where % removal of Fe-Al-Zr in removing Cd(II), Cr(VI) and Pb(II) were calculated. Figure 12 shows the % removal of the heavy metals in the absence of $NaNO_3$, removal Cd(II),

Cr(VI) and Pb(II) were 99.8, 93 and 94%, respectively and in the presence of 0.1 M $NaNO_3$, the % removal were observed to decrease to 96.05, 87 and 82% for Cd(II), Cr(VI) and Pb(II), respectively. As the concentration of $NaNO_3$ increases, the % removal was decreased due to the accumulation of charge in the vicinity of the Fe-Al-Zr surfaces. Upon addition of $NaNO_3$, the cation Na^+ would be distributed in the outer layer surrounding the Fe-Al-Zr ternary nanocomposite sorbent.

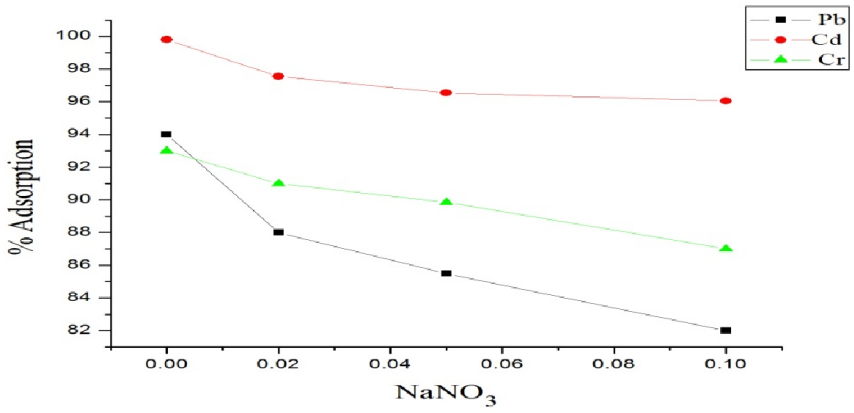

Figure 12. Effect of ionic strength on % removal of Cd(II), Cr(VI) and Pb(II) in a ternary system.

A high $NaNO_3$ concentration indicates more Na^+ ions exist in the outer layer which would exert a strong repulsive force that repels the approaching metal ions such as Cd(II), Pb(II) and Cr(VI) leading to a decrease in the %removal of Fe-Al-Zr ternary nanocomposite sorbent. But further increase in ionic strength can compress the electric double layer on surface of adsorbents, reducing its electrostatic attraction to Cr(VI) (Xiaoshu *et al.,* 2013). The effect of ionic strength on the uptake capacity of Fe-Al-Zr ternary nanocomposite sorbent would also distinguish between formation of inner sphere and outer sphere complexes. A cation can be adsorbed on the Fe-Al-Zr surface as an inner sphere or an outer sphere complex. Outer sphere complexes involve weak, electrostatic interaction and are strongly affected by the changes in the ionic strength of the solution. Outer sphere complexes are more sensitive to changes in the ionic strength of the solution since electrolyte ions are placed in the outer plane surrounding the solid phase (adsorbent) along with the outer sphere complexes. On the other hand, inner sphere complexes form strong chemical bonds such as covalent or ionic binding and are weakly affected by the ionic strength (Cybelle *et al.,* 2012).

In other words, the adsorption process was hindered in part by excess Na^+ in the solution. Metal ions usually form electric double layer (EDL) complexes with Fe-Al-Zr ternary nanocomposite sorbent. It has been reported (Samia *et al.,* 2012) that the presence of a cation, such as Na^+, decreases heavy metal ion interaction constants due to the accumulation of charge in the vicinity of the Fe-Al-Zr surfaces. The presence of these cations creates a localized potential that repels other cations, thus reducing the adsorption potentials of the Fe-Al-Zr. Additionally, the ionic strength affected the activity coefficients of Cd(II), Cr(VI) and Pb(II) ions, which limited their transfer to the Fe-Al-Zr ternary nanocomposite sorbent surfaces. Moreover, an increase in ionic strength supplies more positive ions that compete with the heavy metal ions for adsorption sites on the Fe-Al-Zr ternary nanocomposite sorbent.

4.6. Effect of Interfering Ions

The effects of potential interferences occurring in water samples on the determination of Pb(II), Cd(II) and Cr(VI) were investigated using the optimized batch procedure. The reliability of the method has to be examined in presence of possible matrix effects because the interference ions affect the adsorption of target analyte. The effect of other ions like Na+, K^+, Ca^{2+}, Mg^{2+} and Fe^{3+} on the adsorption process was studied at the same concentrations with Pb(II), Cd(II) and Cr(VI) ion. The ions were added to 20 mg/L of metal ion solutions and the contents were agitated for 6 h for Pb(II), Cd(II) and 12 h Cr(VI) at 25^{o}C. The results showed in the Figure 13, Fe^{3+} affect the percentage of adsorption of metal ion on Fe-Al-Zr nanocomposite, since the interaction of Fe^{3+} at available sites of adsorbent through competitive adsorption is so effective. While Na+, K^+, Ca^{2+}, Mg^{2+} ions the interference of these ions at available surface sites of the sorbent through competitive adsorption also low.

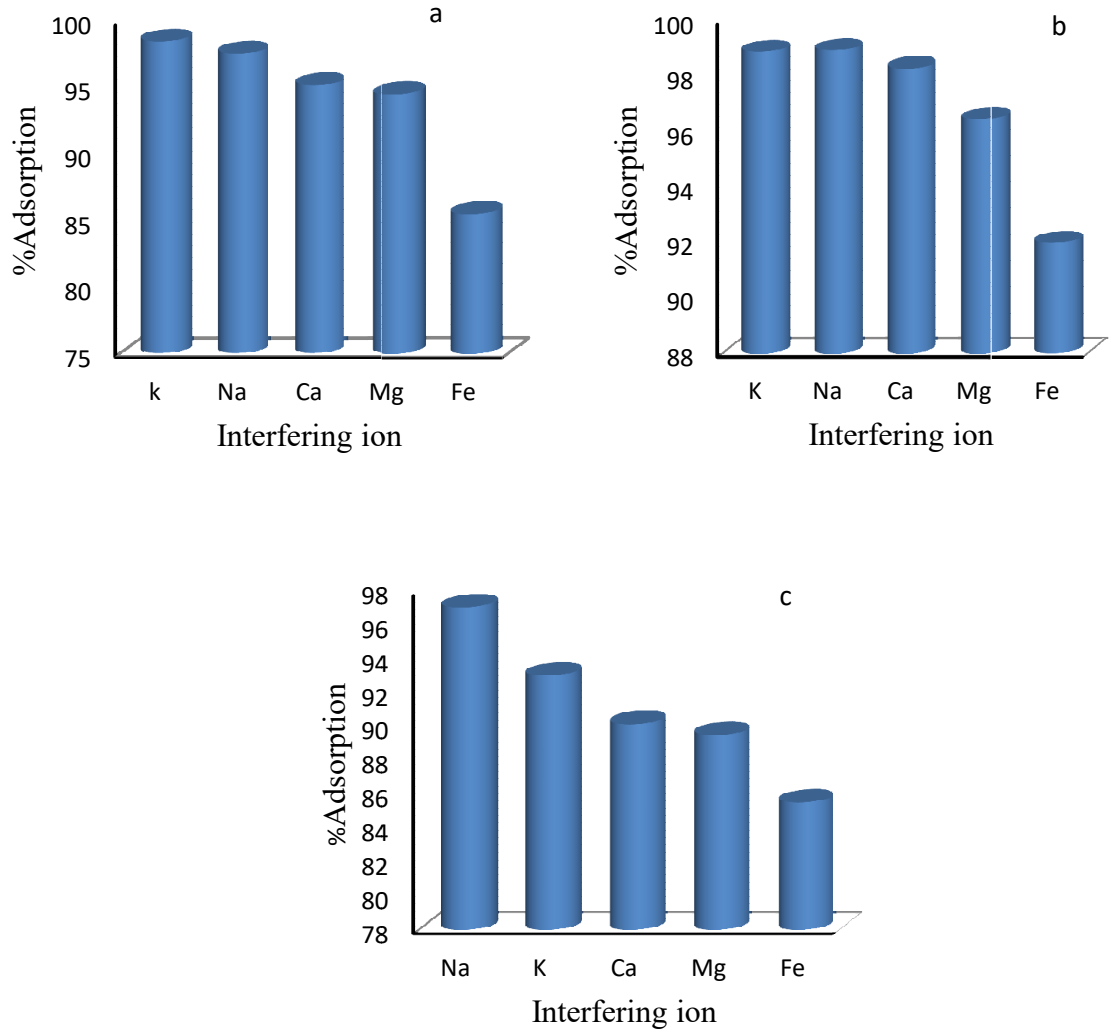

Figure 13. Effect of interfering ion (a, b, and c) for % removal of Pb(II), Cd(II) and Cr(VI), respectively, in a ternary system.

4.7. Desorption Study

The lead, chromium and cadmium desorbability can be defined as the ratio of the desorbed Cd(II), Cr(VI) and Pb(II) ions over the total adsorbed Cd(II), Cr(VI) and Pb(II) ions by the adsorbent. Therefore, the desorbability can be used to indicate the degree of Cd(II), Cr(VI) and Pb(II) ions desorption from the adsorptive materials (Zeng *et al.,* 2004).

As figure 14 shows that the desorption of metal ion increases from 9.71to 32.1% for Cd(II), 16.4-60% for Cr(VI) and from 28.5 to 39.3% for Pb(II) as pH of the solution increases from 2 to

9. These result indicates that desorption is more favorable at higher pH in case of adsorbate ions. Up to pH 6 the desorption of adsorbate ions take place slightly, then after that increased highly. When compared to Pb(II) and Cr(VI) desorption of Cd(II) is more difficult than Pb(II) and Cr(VI) at low pH. For Cd(II), Cr(VI) and Pb(II) ions maximum desorption was obtained at PH 9 (32.1%, 60% and 39.3%) for Cd(II), Cr(VI) and Pb(II), respectively.

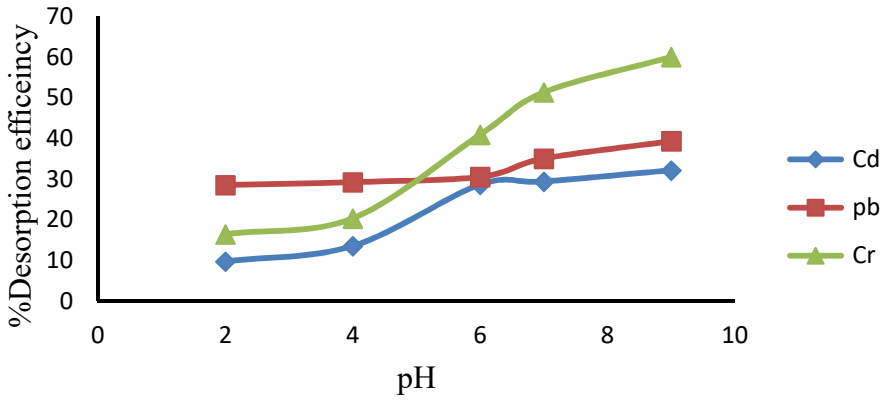

Figure 14. Effect of pH on desorption of Cd(II), Cr(VI) and Pb(II) ions in, nanoparticle mixed oxide of Al-Fe-Zr, respectively at varied pH.

4.8. Recycling of Fe-Al-Zr

The recycling and regeneration ability is significant for the practical application of adsorbents. Such adsorbents have excellent adsorption capacity as well as high desorption property will reduce secondary pollution and the overall cost. Thus, the desorption experiments of Fe-Al-Zr were performed to evaluate the recyclability of the sorbent. The used adsorbents were washed by base sodium hydroxide as eluent, and the adsorbed Cd(II), Pb (II) and Cr(VI) ions molecules could be efficiently desorbed. The results of four consecutive adsorption–desorption cycles were shown in Fig. 15. It can be seen that the adsorption capacity of Cd(II), Pb (II) and Cr(VI) ions adsorbed on as-prepared adsorbent slightly decreased after every cycle of adsorption–desorption process. Therefore, the as-prepared magnetic nanocomposite are expected to be employed repeatedly and cost-effective in metal ion wastewater treatment.

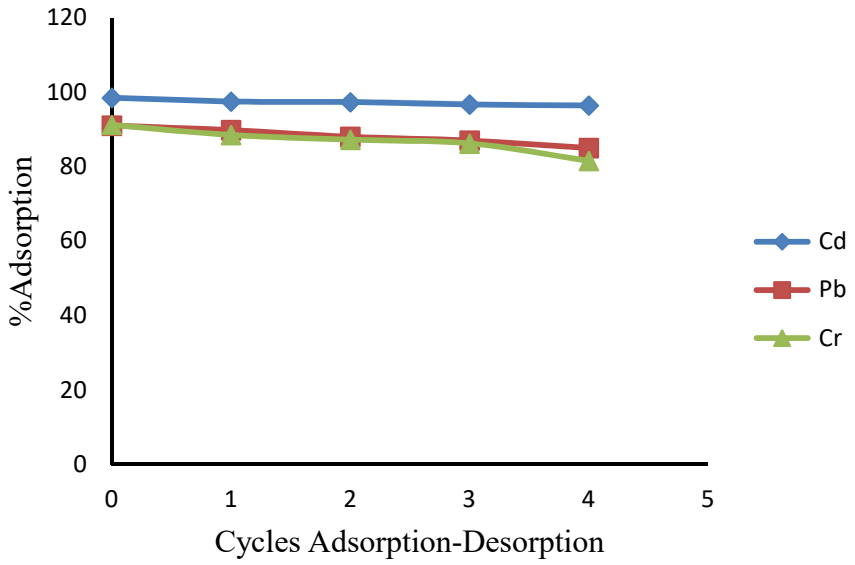

Figure 15. Cycles of adsorption-desorption for the reuse of Fe-Al-Zr as adsorbents for Cd(II), Pb(II) and Cr(VI) removal.

4.9. Comparison of the Method with Others

Toward the comparison of analytical performance of the nanosorbent with that of other sorbents. Some comparative adsorption data are present in Table 4. Adsorption capacities obtained are comparable to those presented by other methods. The present work has relatively high adsorption capacity when compared to literature report Małgorzata and Lidi (2014), Mahdavian (2010), Huang and Chen (2009); Xiaoyao *et al.,* (2014). However, the proposed method is simpler than the others. For example, there is no need to use any complexing and/or chelating agent and the adsorbent is stable with a recycling period greater than chelating agent without major loss in its quantities and metal recovery property.

Table 4. Comparative data for various adsorption methods.

Adsorbents	Analyte	Adsorption Capacity (mg/g)	Determination technique	Ref.
Glauconite	Cd(II) Pb(II)	3.44 9.12	FAAS	Małgorzata and Lidia, 2014
Amino-modified Fe_3O_4 MNPs	Cr(VI)	12.43	-	Mahdavian, Mirrahimi, 2010
m-PAA-Na-coated MNPs	Cd(II)	5	-	Huang and Chen, 2009
Fe_3O_4-GS	Cr(VI)	17.29	-	Xiaoyao *et al.,* 2014
Al-Fe-Zr	Cd(II) Cr(VI) Pb(II)	4.38 26.8 9.44	FAAS	This work

5. SUMMARY, CONCLUSIONS AND RECOMMENDATIONS

5.1. Summary and Conclusions

Fe-Al-Zr ternary nanocomposite adsorbent was synthesized by co-precipitation method. The percentage compositions of Fe, Al, Zr were 72.3, 23.9 and 3.8, respectively. Laboratory experiments were carried out to investigate adsorption kinetics and equilibrium in batch mode. The surface structure of this oxide was investigated using FT-IR, BET and XRD. In the adsorption test, pH effect, adsorbent dose, contact time, agitation speed, initial metal ion concentration, adsorption isotherms, kinetics, desorption, thermodynamics, ion strength, recycling, pH_{PZC} and interfering ion adsorption were examined. The optimum values obtained for these parameters (pH effect, adsorbent dose, contact time, agitation speed and initial concentration) were, (6, 4 and 6), (1, 0.1, and 0.5) g, (12, 12 and 6) h, (120,120 and 100) rpm and 20 ppm, respectively.

FT-IR spectrometry shows the surface functional groups of the adsorbent before and after adsorption of metal ion. BET is also show the surface area (205 m^2/g) of adsorbent as well as the X-ray diffraction pattern indicated that all the as-synthesized materials are in the nano range. The Cd(II), Cr(VI) and Pb(II) ions removal by this ternary nanocomposite was highly pH dependent, with a maximum retention of Cd(II), Cr(VI) and Pb(II) ions occurred at pH-6, 4 and 6, respectively. At low initial concentration of Cd (II), Cr(VI) and Pb(II) metals ions are adsorbed by specific active sites, while at higher concentrations; lower adsorption yield obtained due to the saturation of adsorption sites. Pseudo second-order reaction rate model adequately described the kinetics of sorption of Cd(II), Cr(VI) and Pb(II) ions with high coefficient of determination (R^2 = 0.9958, 0.9998 and 0.9967). The adsorption isotherms of Cd(II), Cr(VI) and Pb(II) ions were analyzed using both Freundlich and Langmuir isotherm models. Freundlich equations were fitted more for the adsorption process relative to Langmuir. Values of the equilibrium parameter (R_L) from Langmuir isotherm and n values from the Freundlich isotherm have indicated that the adsorption process is favorable. The sorption property of the nanocomposite mixed oxide adsorbent has also been treated with respect to thermodynamic parameters viz. ΔG, ΔS and ΔH. The Cd(II), Cr(VI) and Pb(II) ions sorption process was found to be spontaneous and endothermic from the negative and positive values of ΔG and ΔH respectively. The positive

value of ΔS showed the increased randomness at the solid/solution interface. Cd(II), Cr(VI) and Pb(II) ions desorbability was observed to increase with increasing pH indicating that relatively favorable conditions for repeatability of the process at higher pH values. Furthermore, effect of co-existing cation has also been investigated and the adsorbent is still found to be efficient for Cd(II), Cr(VI) and Pb(II) ions removal.

5.2. Recommendations

The result of the nano-sized ternary mixed oxide adsorbent indicates that the adsorbent is capable of removing metal ions from aqueous solution. Therefore, the following recommendations are made as a result of the outcome of this study:

- Investigate further about the effects or influences of adsorbents' pore size (morphological study) and temperature that influences the sorption process.
- Carry out the research on the removal capacity of this nanosorbent for other anions like arsenite/arsenate and Uranium.
- Optimize the removal efficiency of the nano sized adsorbent through continuous column experiment.
- To conduct a research on quaternary mixed metal oxides nanocomposite adsorbent to further enhance the sorption efficiency.

6. REFERENCES

Abdus-salam, N., Adekola, F.A. 2005. The influence of pH and adsorbent concentration on adsorption of Pb and Zn on a natural goethite. *African Journal of Science and Technology*, 6: 55-66.

Abia, A.A. and Asuquo, E.D. 2008. Sorption of Pb(II) and Cd(II) ions onto chemically unmodified and modified oil palm fruit fibre adsorbent: Analysis of pseudo second order kinetic models. *Indian Journal of Chemical Technology*, (15): 341-348.

Amiri, M., Fadaei, J., Baghvand, E.A. and Ezadkhasty, Z. 2014. Removal of Heavy Metals Cr (VI), Cd (II) and Ni (II) from Aqueous Solution by Bioabsorbtion of Elaeagnus Angustifolia. *International Journal of Environmental Research, 8(2): 411-420.*

Anbiaa, M., Kargoshab, K. and Khoshbooeic, S. 2015. Heavy metal ions removal from aqueous media by modified magnetic mesoporous silica MCM-48. *Chemical Engineering Research and Design* 9 3: 779–788.

Anqi, W., Xiang, L., Zhongxing S. and Huanwang J. 2014. New magnetic nanocomposites of ZrO_2–Al_2O_3–Fe_3O_4 as green solid acid catalysts in organic reactions. *Catalysis Science & Technology,* 4: 71-80.

Bamlaku Semagne, Isabel, D., Tesfahun Kebede, Abi M. Taddesse. 2016. Synthesis, characterization and analytical application of polyaniline tin(IV) molybdophosphate composite with nanocrystalline domains. *Reactive and Functional Polymers*, 98: 17–23.

Bhatnagar, S.P. and Rosensweig, R.E. 2001. Sonochemical Synthesis of Functionalized Amorphous Iron oxide nanoparticles. *Journal of Magnetism Magnnetic Materials Langmuir*.17: 5093-5097.

Barakat, M.A., Al-Ansari, A.M., Kumar, R. 2016. Synthesis and characterization of Fe−Al binary oxyhydroxides/MWCNTS nanocomposite for the removal of Cr(vi) from aqueous solution. *Journal of the Taiwan Institute of Chemical Engineers, 63(303-311).*

Buzuayehu Abebe, 2012. Synthesis, characterization and sorption property of nano sized iron/alumina/manganese mixed oxide sorbent system for removal of phosphate from aque ous solution. MSc Thesis, Haramaya University.

Carp, O., Huisman, C.L. and Reller, A. 2004. Photoinduced reactivity of titanium dioxide. *Progress in Solid State Chemistriy,* 32(1-2): 33-177.

Castro-González, M.I. & Méndez-Armenta, M. 2008. Heavy metals: Implications associated

Chanani, M.E., Bahramifar, N., Younesi, H. 2015. Synthesis of Fe_3O_4@silica core–shellparticles and their application for removal of copper ions from water. *Journal of Applied Research in Water and Wastewater* 4: 176-182.

Chen, X. and Mao, S.S. 2007. Titanium dioxide nanomaterials: synthesis, properties, modifications and applications. *Chemical Review,* 107(7): 2891-2959.

Corr, S.A. 2013. Metal oxide nanoparticles. *Nanoscience* (1): 180–234.

Cristina, Q., Zélia, R., Bruna, S., Bruna, F., Hugo, F., Teresa, T. 2009. Removal of Cd(II), Cr(VI), Fe(III) and Ni(II) from aqueous solutions by an E. col biofilm supported on kaolin. *Chemical Engineering Journal*, 149: 319–324.

Cybelle, M.F., Wan-Chi, T., Shiow-Shyung, L., Maria, L.D. and Meng-Wei, W. 2012. Copper, nickel and lead adsorption from aqueous solution using chitosan-immobilized on bentonite in a ternary system. *Sustaining Environmental Resources,* 22(6): 345-355.

Dada, A.O., Olalekan, A.P., Olatunya, A.M., DADA, O. 2012. langmuir, freundlich, temkin and dubinin–radushkevich isotherms studies of equilibrium sorption of Zn^{2+} unto phosphoric acid modified rice husk. *Journal of Applied Chemistry,* 3: 38-45.

David, W.O., Colin, B.H. and Thomas, F.O. 2008. Heavy metals adsorbents prepared from the modification of cellulose. *Biosource Technology*, 99: 6709-6724

Dimple, L. 2014. Adsorption of heavy metals: A review. *International Journal of Environmental Research and Development*. 4 (1): 41-48.

Duruibe, J.O. ,Ogwuegbu, M.O.C. and Egwurugwu, J.N. 2007. Heavy metal pollution and human biotoxic effects. *International Journal of Physical Sciences* 2(5): 112-118

Fekadu Kassahun Bahiru, 2015. Synthesis and characterization of $Al_2O_3/Fe_3O_4/ZrO_2$ heterojunction ternary oxides nanocomposite for nitrate sorption from aqueous solution. MSc. Thesis, Haramaya university.

Fettea, C.W. 1999. Contaminant Hydrogeology, Second Edition, Prentice-Hall Publishing Company, Upper Saddle River NJ. 500p.

Figueroa, E. (2008). Are more restrictive food cadmium standards justifiable health safetymeasures or opportunistic barriers to trade.An answer from economics and public health. *Science of the Total Environment,* 389: 1-9.

Franus, M. and Bandura, L. 2014. Sorption of heavy metal ions from aqueous solution by Glauconite. *Fresenius Environmental Bulletin,* 23(3a): 40; 20-618.

Freundlich, H., 1906. Über die adsorption in lösungen. Zeitschrift für physik. *Chemie,* 57:385-470.

Giraldo, L., Erto, A., Moreno-Piraja, ´n J. C. 2013. Magnetite nanoparticles for removal of heavy metals from aqueous solutions: synthesis and characterization. *Adsorption,* 19: 465–474.

Gottipati, R. and Mishra, S. (2012). Application of response surface methodology for optimization of Cr(III) and Cr(VI) adsorption on commercial activated carbons. *Research Journal of Chemical Sciences*, 2(2): 40-48.

Gupta, V.K. and Nayak, A. 2012. Cadmium removal and recovery from aqueous solutions by novel adsorbents prepared from orange peel and Fe_2O_3 nanoparticles. *Chemical Engineering Journal,* 180, 81-90.

Haddad, P.S. and Seabra, A.B. 2013. Biomedical applications of magnetic nanoparticles. In iron oxides: structure, properties and applications; Martinez, A.I., Ed. *Nova Science*, 1: 165–188.

Hadjmohammadi, M.R., Salary, M. and Biparva, P. 2011. Removal of Cr (VI) from aqueous solution using pine needles powder as a biosorbent. *Journal of Applied Sciences in Environmental Sanitation,* 6 (1): 1-13.

Harrison, N. (2001). Inorganic contaminants in food, In: Food Chemical Safety Contaminants Watson, D.H. (Ed.), 1:148-168.

Ho, Y.S. (1995) *Ph.D. Thesis, Univ. Birmingham, Birmingham, U.K*.

Huang, S.H, Chen, D.H. 2009. Rapid removal of heavy metal cations and anions from aqueous solutions by an amino-functionalized magnetic nano-adsorbent. *Journal of Hazardous Material*, 163(1): 174–9.

Ingrid, C. and Jamie, B. 1999. Toxic cyanobacteria in water: a guide to their public health consequences, monitoring, and management. *E & FN Spon, London, New York*. ISBN 1-85573-462-1.

John, C., Crittenden, N. and Montgomery, W.H. 2005. Water treatment principles and design. *John Wiley, Hoboken, N.J., 2nd edition,* 685p.

Julio, D.A., Alberto F.A., Ignacio R.G., Merced M., and Tomas V. 2012. Synthesis and characterization of alumina-Zirconia powders obtained by sol-Gel method: Effect of solvent and water addition rate. *Materials Sciences and Applications,* 3: 650-657.

Kaewsarn, p., Saikaew, W.A. and Wongcharee, S. 2008. Dried biosorbent from banana peel: A potential biosorbent for removal of cadmium ions from aqueous solutions. The 18th thailaand chemical engineering and applied chemistry conference, pattaya thailand.

Kadirvelu, K. and Namasivayam, C. 2000. Agricultural by-products as metal adsorbents: Sorption of lead(II) from aqueous solutions onto coirpith carbon. *Environmental Technology*, 21: 1091- 1097.

Keshmiri, M., Troczynski, T. and Mohseni, M. 2006. Properties of amorphous and crystalline titanium dioxide from first principles. J*ournal of Hazardous Materials, 128*-130.

Khazaei, I., Aliabadi, M. and Mosavian, H.H.T., 2011. Use of agricultural waste for removal of Cr(VI) from aqueous solution. *Iranian Journal of Chemical Engineering*, 8: 4.

Kuchibhatla, V.N.T.S., Karakoti, A.S., Seal, S.D. 2007. One dimensional nanostructured materials. *Progress in Materials Science*, 52(5): 699-913.

Kulkarni, S.A., Sawadh, P. S. and Kokate, K. K. 2012. Synthesis and Characterization of Fe_3O_4 Nanoparticles for Engineering Applications. *International Journal of Computer Applications,* 17-18.

Kwon, J.S., Yun, S.T., Lee, J.H., Kim, S.O., Jo, H.Y. (2010). Removal ofdivalent heavy metals (Cd, Cu, Pb, and Zn) and arsenic (III) from aqueoussolutions using scoria: kinetics and equilibrium of sorption, J*ournal of Hazardous Materials,* 174, 307–313.

Langmuir, I., 1918. The adsorption of gases on plane surfaces of glass, mica and platinum. *Journal of the American Chemical Society*, 40(9): 1361–1403.

Langmuir, D. 1978. Uranium solution-mineral equilibrium at low temperatures with applications to sedimentary ore deposits. *Geochemical et Cosmochimica Acta,* 42: 547-569.

Mahdavian, A.R and Mirrahimi M.A.S. 2010. Efficient separation of heavy metal cations by anchoring polyacrylic acid on superparamagnetic magnetite nanoparticles through surface modification. *Chemical Engineering of Journal*. 159(1–3): 264–71.

Mansoori, G.A., Rohani, T., Bastami, A., Ahmadpour, Z. and Eshaghi 2008. Environmental application of nanotechnology. *Annual Review of Nano Research, (2) Chap.2: 1-73.*

Mengel, K., Kirkby, E.A. 1978. Principles of plant nutrition, *International Potash Institute, Berne, Switzerland*, (11): 367-519.

Michael, M.c. 1992. Isothermal entropy changes in nanocomposite. *Journal of Magnetism and Magnetic Materials,* 11- 29.

Mina, G., Hassan, H. and Maryam, M. 2011. Hexavalent chromium removal from aqueous solution via adsorption on granular activated carbon: adsorption, desorption, modeling and simulation studies. *ARPN Journal of Engineering and Applied Sciences,* 6(9): ISSN 1819-6608.

Ming-Ho, Y. (2005). Environmental toxicology: biological and health effects of pollutants. Chap. 12, CRC Press LLC, ISBN 1-56670-670-2, 2nd Edition, BocaRaton, USA.

Mousavi, H. Z., Hosseynifar, A., Jahed, V. and Dehghani, S. A. M. 2010. Removal of lead from aqueous solution using waste tire rubber ash as an adsorbent. *Brazilian Journal of Chemical Engineering*, 27(01): 79 – 87.

Mulu, B. D. 2013. Batch Sorption Experiments: langmuir and freundlich isotherm studies for the adsorption of textile metal ions onto teff straw (*Eragrostis tef*) agricultural waste. *Journal of Thermodynamics,* 1-7.

Netzer, A. and Wilkinson, P., 1974. "Removal of heavy metals from wastewater by adsorption on sand," in Proceedings of the *29th Industrial Waste Conference*, 29: 841.

Oskam, G. 2006. Metal oxide nanoparticles: synthesis, characterization and application., J Sol-Gel SciTechn (2006) 37: 161–164.

Panumati, S., Chudecha, K. and Vankhaew, P. 2008. Adsorption of phenol from dilutedaqueous solutions by activated carbons obtained from bagasse, oil palm shell and pericarp of rubber fruit. *Journal of Science Technology,* 30: 185-189.

Poon, C.P.C. 1986. Removal of Cd (II) from wastewaters. In cadmium in the environment, mislin, H., Raverva, O., Eds.;Birkhauser: Basel, Switzerland; 6–55.

Raka, M. and Sirshendu, D. 2014. Adsorptive removal of nitrate from aqueous solution by polyacrylonitrile–alumina nanoparticle mixed matrix hollow-fiber membrane. *Journal of Membrane Science*, 466: 281– 292.

Salmani, M.H., Zarei, S., Ehrampoush M.H., Danaie, S. 2013. Evaluations of pH and high ionic strength solution effect in cadmium removal by zinc oxide nanoparticles. *Journal of Applied Science Environmental Management* 17 (4): 583-593.

Samia, A. Kosaa, Ghalia Al-Zhrania, Mohamed Abdel Salama 2012. Removal of heavy metals from aqueous solutions by multi-walled carbon nanotubes modified with 8-hydroxyquinoline. *Chemical Engineering Journal,* 181–182 : 159–168.

Satish, P., Vaijanta, D., Sameer, R. and Naseema, P. 2011. Kinetics of adsorption of crystal violet from aqueous solutions using different natural materials. *International Journal of Environmental science,* 1: 6.

Shafi, K. V. 2002. Building blocks for nanotechnology. *Chemistry of Materials. 14*: 1778

Sharma, Y.C. 2008. Thermodynamics of removal of cadmium by adsorption on indigenous clay. *Chemical Engineering Journal,* 145: 64–68.

Shrimant, V.R., Haresh, P., Satish, B. A. and Sandip, D.M. 2015. Adsorption and desorption studies of cadmium (ii) ions from aqueous solutions onto tur pod (*Cajanus cajan*). *International Journal of Advanced Chemical Research,* 4 (5): 030-038.

Simone, M., Fernando, G.C. and Maria D.L.P. 2012. Heavy metals and human health. *Environmental Health - Emerging Issues and Practice, 228-324.*

Suryanarayana, C. 1995. Nano crystallinematerials. *International Materials Reviews*, 40(2): 41-64.

Suryanarayana, C. 2002. The structure and properties of nanocrystalline materials: Issues and concerns. *Journal of the Minerals, Metals and Materials Society*, 54(9): 24-27.

USEPA. 2007. Nanotechnology white paper. ERA 100/B-07/001. Washington, DC20460. Science Policy Council, U.S. *Environmental Protection Agency,* 1-119.

Vatutsina, O.M., Soldatov, V.S., Sokolova, V.I., Johann, J., Bissen, M. and Weissenbacher, A. 2007. A new hybrid (polymer/inorganic) fibrous sorbent for arsenic removal from drinking water. *Reactive and Functional Polymers,* 67: 184-201.

Vijayakumar, G., Tamilarasan, R. and Dharmendirakumar, M. 2012. Adsorption**,** kinetic, equilibrium and thermodynamic studies on the removal of basic dye rhodamine-b from aqueous solution by the use of natural adsorbent perlite. *Journal of Maternal Environmental Science,* 3 (1): 157-170.

Waalkes, M.P. 2000. Cadmium carcinogenesis in review. *Journal of Inorganic and Biochemistry*, 79: 241–244.

Wang, X., Guo, Y., Yang, L., Han, M., Zhao, J. and Cheng, X. 2012. Nanomaterials as sorbents to remove heavy metal ions in wastewater treatment. *Environmental & Analytical Toxicology*, 2(7): 1-7.

Wang, J.S., Hu, X.J., Wang, J., Bao, Z.L., Xie, S.B. and Yang, J.H. 2014. The tolerance of rhizopusarrihizus to U(VI) and biosorption behavior of U(VI) onto R.arrihizus. *Biochemical Engineering Journal.* 51:19–23.

Watson, S., Beydoun, D., Scott, J. and Amal, R. 2004. Preparation of nanosized crystalline TiO_2 particles at low temperature for photocatalysis. *Journal of Nanoparticle Research*, 6: 193-207.

Wei, C., Jiaqi, W. 2007. Facile synthesis of superparamagnetic magnetite nanoparticles in liquid polyols. *Journal of Colloid and Interface Science,* 305: 366–370.

Xiaoshu, Lv., Yunjun Hu., Jie T., Tiantian, S., Guangming, J., Xinhua Xu. 2013. Effects of co-existing ions and natural organic matter on removal of chromium (VI) from aqueous solution by nanoscale zero valent iron (nZVI)-Fe3O4 nanocomposites. *Chemical Engineering Journal,* 218: 55–64.

Xiaoyao, G., Bin, D., Qin, W., Jian, Y., Lihua, H., Liangguo, Y., Weiying, X., 2014. Synthesis of amino functionalized magnetic graphenes composite material and its application to remove Cr(VI), Pb(II), Hg(II), Cd(II) and Ni(II) from contaminated water. *Journal of Hazardous Materials,* 278: 211–220.

Yadanaparthi, S.K.R., Graybill, D. and Wandruszka, R. (2009). Adsorbents for the removal of arsenic, cadmium, and lead from contaminated waters. *Journal of Hazardous Material.,* 171: 1-15.

Yanga, G., Tanga, L., Leia, X., Zenga, G., Ye, C., Xue, W., Yaoyu, Z., Sisi, L., Yan, F., Yi, Z. 2014. Cd(II) removal from aqueous solution by adsorption on α-ketoglutaricacid-modified magnetic chitosan guide. *Applied Surface Science,* 292: 710– 716.

Yanjun, D., Yanju, Z., Baoan, D. and Jingfeng, Z. 2008. Preparation of nano sized $ZnFe_2O_4$ powders by co-precipitation method. 10(10): 52

Yin, H., Wada, Y., Kitamura, T., Kambe, S., Murasawa, S., Mori, H., Sakata, T. and Yanagida, S. 2001. Properties of amorphous and crystalline titanium dioxidefrom first principles. *Journal of Materials Chemistry,* 11(6): 1694.

Yohannes, A. 2014. Biosupported Fe-Al-Mn ternary oxide nanosorbent: synthesis, characterization and lead (ii) sorption property in aqueous solution. MSc Thesis, Haramaya University, Haramaya, Ethiopia.

Yu, JW., Neretnieks, I. 1990. Single-component and multicomponent adsorption equilibrium on activated carbon of methylcyclohexane, toluene, and isobutyl methyl ketone. *Industri Engineering Chemistry Research* 29: 220–231.

Zhao, G., Wu, X., Tan, X. and Wang, X. 2011. Sorption of Heavy Metal Ions from Aqueous Solutions: A Review. *The open Colloid Science Journal,* 4: 19-31.

Zare, N. E., Lakouraj, M.M., Ramezani, A. 2014. Effective adsorption of heavy metal cations by superparamagnetic poly(aniline-*co*-*m*phenylenediamine)@ Fe_3O_4 nanocomposite. *Advances in Polymer Technology*, 34(3): 1-11.

Zeid, A., Al, O., Ali, H. and Mohamed, A.H. 2011. Kinetic, equilibrium and thermodynamic studies of cadmium (ii) adsorption by modified agricultural wastes. *Molecules*, 16: 10443-10456.

7. APPENDICES

Appendix Table 1. Designation of percentage composition of the as-synthesized powders

Sample Code	Absorbance			Average Conc. (mg/L)		
	Al	Fe	Zr	Al	Fe	Zr
1	0.046	0.613	0.007	3.9±0.188	11.81±0.139	0.618±0.42
2	0.045	0.612	0.008			
3	0.042	0.601	0.005			

Appendix Table 2. Effect of pH on adsorption capacity of nano-sized Fe-Al-Zr mixed oxides

	Cd			Pb			Cr		
pH	Ce(ppm)	%A	qe (mg/g)	Ce(ppm)	%A	qe (mg/g)	Ce(ppm)	%A	qe (mg/g)
2	0.156±0.378	99.5	7.1	1.21±0.2	95.9	7.19	1.51±0.282	94.9	7.12
4	0.096±0.042	99.7	7.476	1.2±0.22	96	7.2	1.1±0.23	96.3	7.2
6	0.034±0.04	99.88	7.49	0.67±0.15	97.76	7.3	1.4±0.36	95.3	7.15
7	0.06±0.032	99.8	7.485	0.74±0.17	97.5	7.32	1.6±0.35	94.67	7.1
9	0.08±0.026	99.7	7.8	0.79±0.168	97.4	7.3	1.8±0.284	94	7.05
11	0.11±0.03	99.6	7.47	0.9±0.23	97	7.27	1.9±0.14	93.67	7.03

Appendix Table 3. Effect of adsorbent dose on adsorption capacity of nano-sized Fe-Al-Zr ternary mixed oxides

	Cd			Pb			Cr		
Dose	Ce(ppm)	%A	qe (mg/g)	Ce(ppm)	%A	qe (mg/g)	Ce(ppm)	%A	qe (mg/g)
0.05	15.4±0.0577	48.67	7.3	9.9±0.45	67	10.05	2.17±0.586	92.7	13.9
0.075	14.74±0.035	50.8	5.1	5.36±0.27	82	8.2	1.4±0.59	95	9.5
0.1	14.71±0.023	50.9	3.8	4.4±0.54	85.3	6.4	1.14±0.466	96.2	7.2
0.5	4.4±0.0577	85.3	1.28	3.7±0.5	87.67	1.3	2.15±0.544	92.8	1.4
1	0.72±0.13	97.6	0.732	8.2±1.2	72.67	0.55	2.2±0.59	92.6	1.39
2	1.03±0.12	96.5	0.36	8.98±0.9	70.1	0.26	2.2±0.585	92.6	1.39

Appendix Table 4. Effect of contact time on adsorption capacity of nano-sized Fe-Al-Zr ternary mixed oxides

	Cd			Pb			Cr		
Time	Ce(ppm)	%A	qe (mg/g)	Ce(ppm)	%A	qe (mg/g)	Ce(ppm)	%A	qe (mg/g)
3	8.03±4.5	73.2	0.55	2.23±0.355	92.6	1.3	8.9±1.15	70	5.3
6	3.5±1.3	88.3	0.66	1.63±0.81	94.6	1.42	7.8±1.04	74	0.56
12	0.35±0.166	98.8	0.74	1.9±0.93	93.67	1.41	1.67±0.76	94.4	7.1
16	1.2±0.476	96	0.72	2.1±0.89	93	1.4	3.2±1.04	89.4	6.7
24	1.6±0.71	94.67	0.71	2.2±0.93	92.67	1.39	4±1	86.67	6.5
48	1.8±0.74	94	0.705	2.367±0.81	92.1	1.38	6±3.04	80	6

Appendix Table 5. Effect of agitation speed on adsorption capacity of nano-sized Fe-Al-Zr ternary mixed oxides

	Cd			Pb			Cr		
Agitation speeed	Ce(ppm)	%A	qe (mg/g)	Ce(ppm)	%A	qe (mg/g)	Ce(ppm)	%A	qe (mg/g)
50	9.3±0.797	69	0.52	4.67±4.1	84.4	1.3	8.4±3.65	72	5.4
100	8.1±3.83	73	0.55	2.72±2.8	90.9	1.36	7.67±3.4	74.4	5.58
120	1.97±1.76	93.4	0.7	3.88±2.9	87.1	1.306	5.56±2.9	81.5	6.1
150	3.8±3.6	87.3	0.655	4.4±2.9	85.33	1.28	7.99±1.32	73.4	5.5
200	5.4±3.99	82	0.62	5.2±3.9	82.67	1.24	8.5±1.3	72	5.37

Appendix Table 6. Effect of Initial lead, Cadmium and Chromium concentration on adsorption capacity of nano-sized Fe-Al-Zr trenary mixed oxides.

	Cd			Pb			Cr		
Conc.(ppm)	Ce(ppm)	%A	qe (mg/g)	Ce(ppm)	%A	qe (mg/g)	Ce(ppm)	%A	qe (mg/g)
10	0.84±0.176	91.6	0.23	0.94±0.069	90.6	0.45	0.36±0.22	96.4	2.4
20	0.67±0.155	96.65	0.48	0.567±0.075	97.2	0.97	0.69±0.21	96.55	4.8
30	2.03±1.12	93.2	0.7	5.8±0.13	80.67	1.21	2.1±1.01	93	6.97
50	5.9±0.32	88.2	1.1	10.22±0.589	79.56	1.98	5.6±0.1	88.9	11.1
100	12.5±1.4	87.5	2.2	21±1.3	79	3.9	13.89±0.3	86	21.5
150	19.1±3.24	87.3	3.3	43.5±1.14	71	5.3	21.4±1.2	85.7	36.9
200	25.4±0.057	87.3	4.4	58.4±1.1	70.8	7.1	29.1±10.3	85.5	42.7

Appendix Table 5. Effect kinetic study on adsorption capacity of nano-sized Fe-Al-Zr trenary mixed oxides.

	Cd					Pb				
C.time	Ce (ppm)	qe (mg/g)	qt (mg/g)	log(qe-qt)	t/qt	Ce (ppm)	qe (mg/g)	qt (mg/g)	log(qe-qt)	t/qt
3	8.03	0.51	0.46	-1.30103	6.5	2.23	1.28	1.2301	-1.3019	2.44
6	3.5	0.61	0.55	-1.22185	10.9	1.63	1.43	1.3686	-1.21183	4.4
12	0.35	0.79	0.7	-1.04576	17.14	1.9	1.46	1.3558	-0.98213	8.85
16	1.2	0.73	0.6	-0.88606	26.67	2.1	1.48	1.3432	-0.86391	11.91
24	1.6	0.82	0.59	-0.63827	40.67	2.2	1.58	1.3305	-0.60293	18.04
48	1.8	1.54	0.64	-0.04576	75	2.367	2.78	1.3118	0.166785	36.6

		Cr		
Ce (ppm)	qe (mg/g)	qt (mg/g)	log(qe-qt)	t/qt
8.9	5.58	5.5	-1.09691	0.5
7.8	5.69	5.6	-1.04576	1.07
1.67	7.46	7.3	-0.79588	1.6
3.2	7.18	7	-0.74473	2.3
4	7.11	6.75	-0.4437	3.6
6	9.21	6.5	0.432969	7.4

Appendix Table 8. Results for Cd(II), Cr(VI) and Pb(II) adsorption isotherms of Fe-Al-Zr trenary nanocomposite mixed oxides.

Pb				
Conc.(ppm)	Ce (ppm)	qe	logce	logqe
10	1.13±0.0577	0.44	0.053	-0.35
20	1.06±0.069	0.95	0.025	-0.022
30	5.8±0.13	1.21	0.76	0.083
50	10.22±0.58	1.98	1.01	0.29
100	21±1.3	3.9	1.32	0.59
150	43.5±1.14	5.3	1.64	0.72
200	58.4±1.1	7.1	1.76	0.85

Cd				
Conc.(ppm)	Ce (ppm)	qe	logce	logqe
20	0.67±0.155	0.48	-0.17	-0.32
30	2.03±1.12	0.7	0.3	-0.15
100	12.5±1.4	2.2	1.1	0.34
150	19.1±3.24	3.3	1.3	0.52

Cr				
Conc.(ppm)	Ce (ppm)	qe	logce	logqe
10	0.36	2.4	-0.44	0.38
20	0.69	4.8	-0.16	0.68
30	2.1	6.97	0.32	0.84
50	5.6	11.1	0.75	1.05
100	13.89	21.5	1.14	1.33

Appendix Table 9. RL values for Cd(II), Cr(VI) and Pb(II) adsorption at different concentration

	Cd	Cr	Pb
Initial conc.(mg/g)	RL	RL	RL
10	0.47	0.32	0.73
20	0.3	0.19	0.58
30	0.23	0.14	0.48
50	0.15	0.084	0.36
100	0.083	0.045	0.22
150	0.06	0.031	0.156
200	0.04	0.023	0.12

Calibration curves

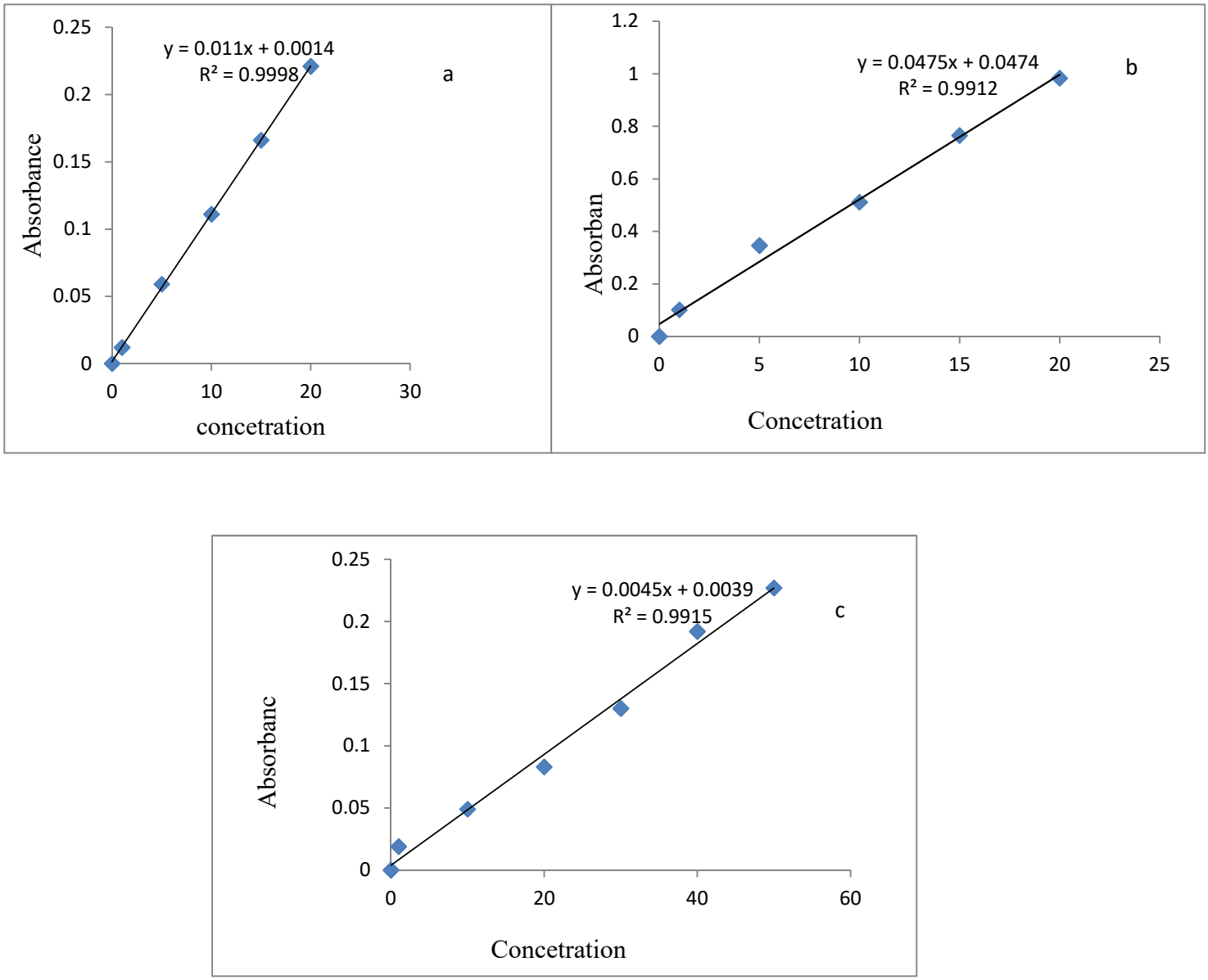

Appendix Figure 1. Calibration curve for Al (a), Fe (b), Zr(c) (FAAS reading).

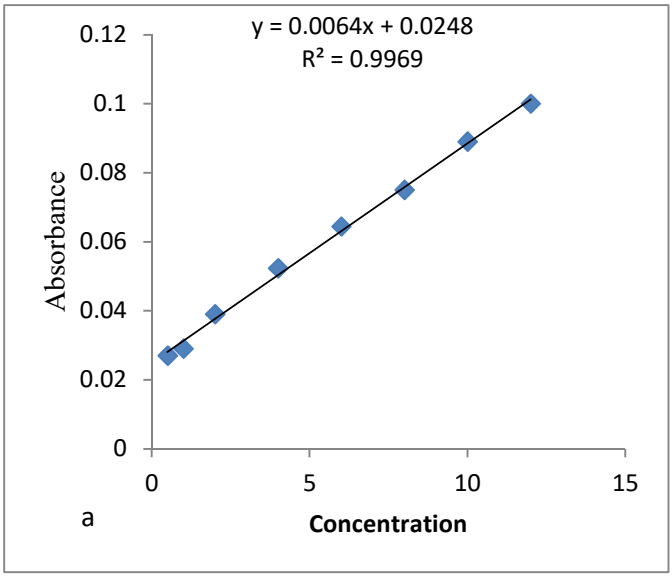

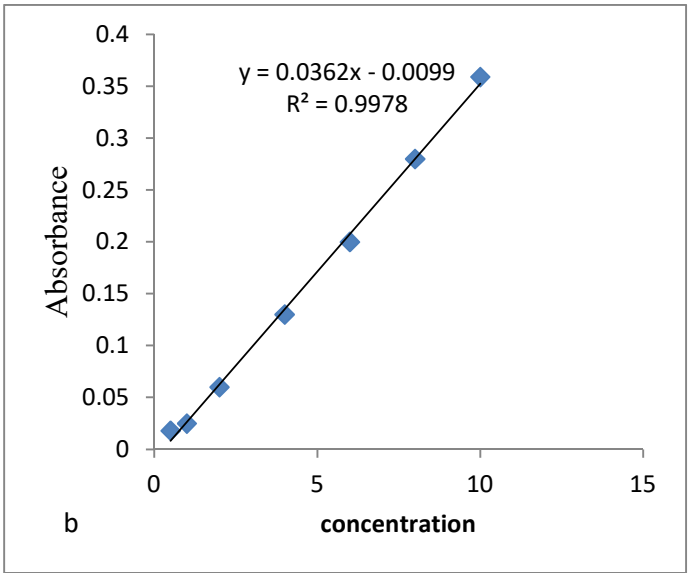

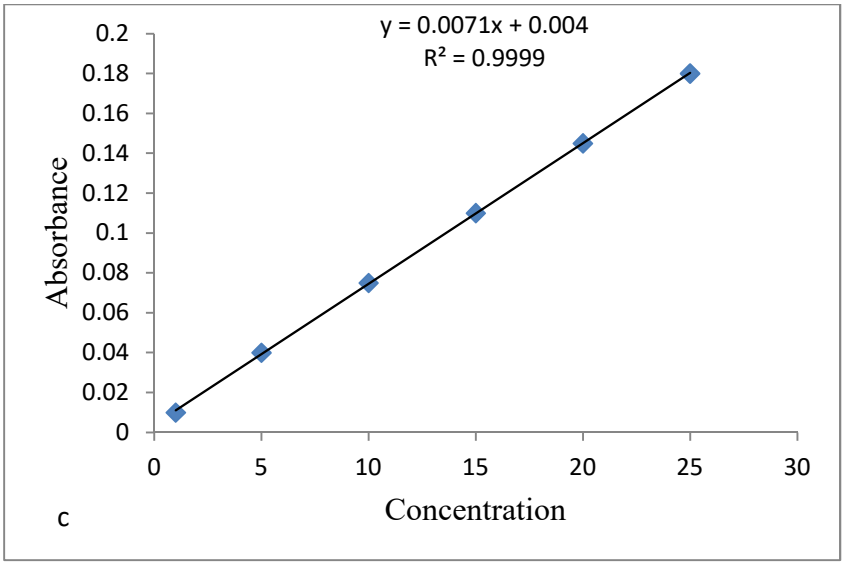

Appendix Figure 2. Calibration curve of Cd(II) for (a), Pb(II) for (b) and Cr(VI) for (c) of pH optimization.

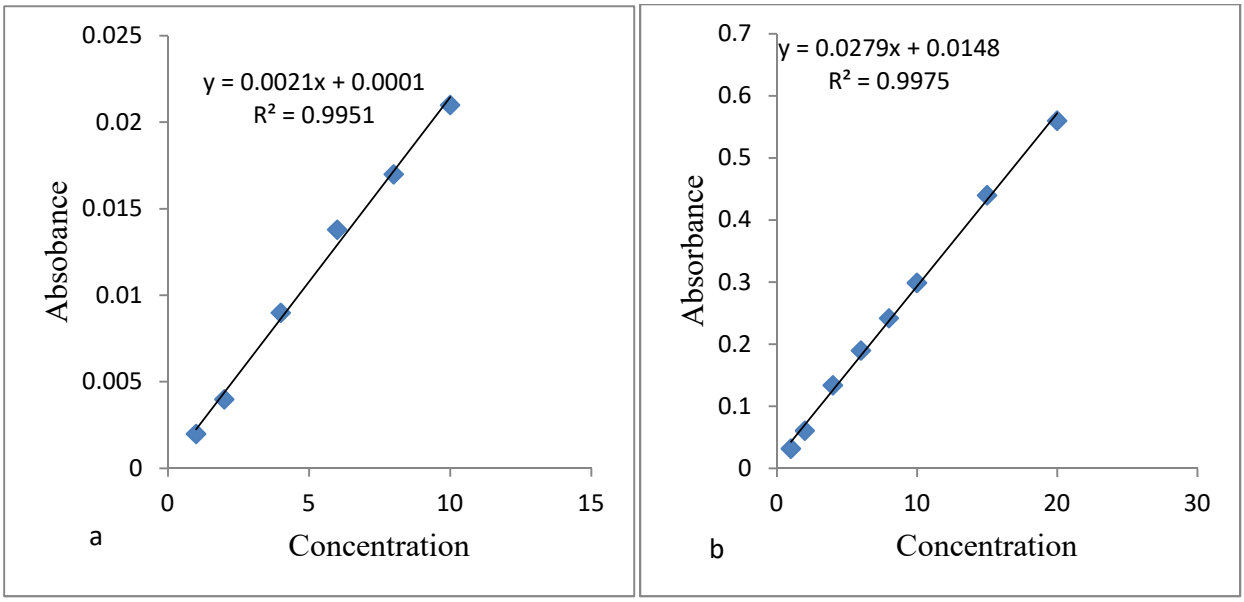

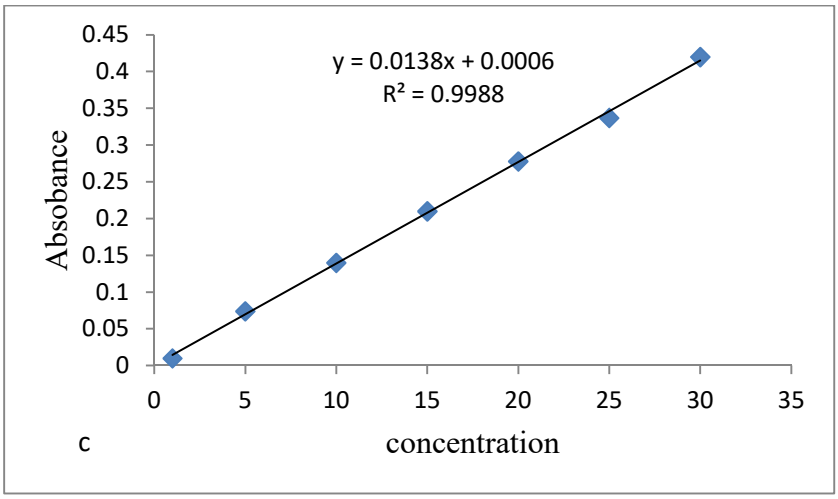

Appendix Figure 3. Calibration curve of Pb(II) for (a), Cd(II) for (b) and Cr(VI) for (c) of Dose optimization.

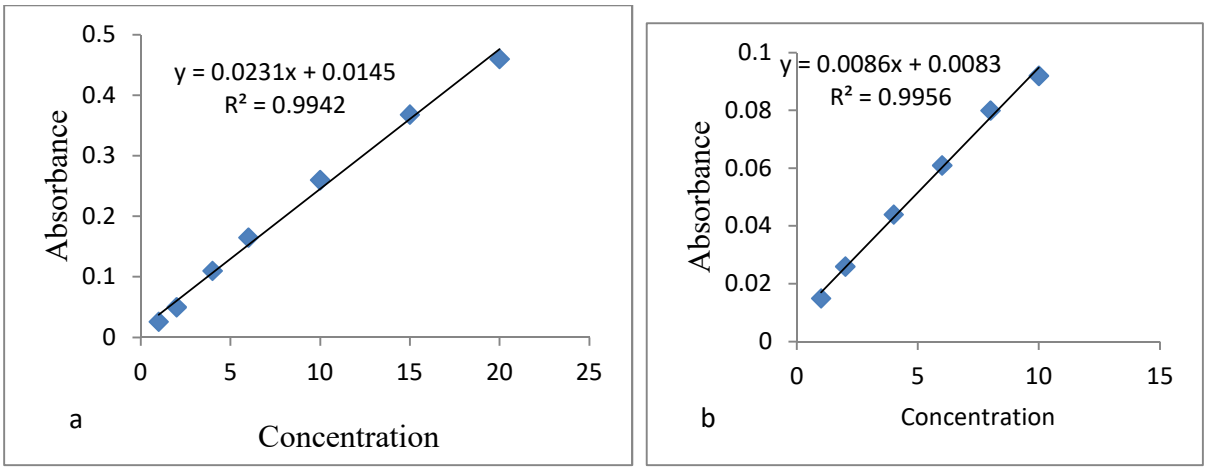

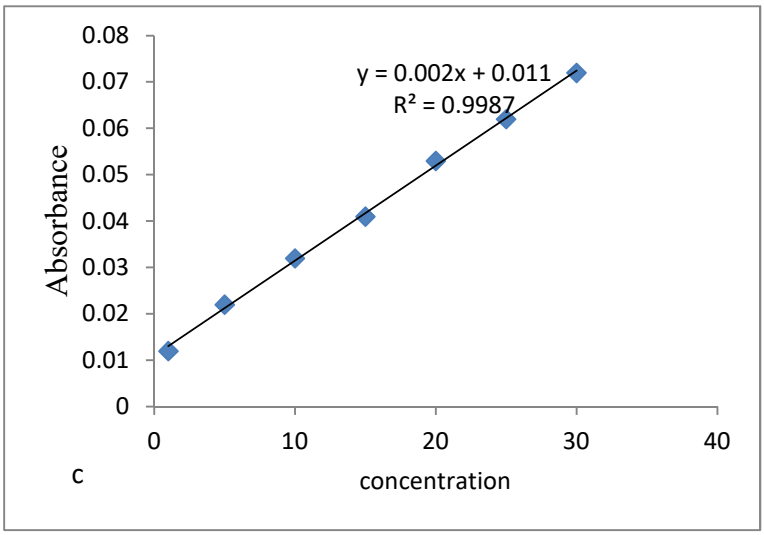

Appendix Figure **4**. Calibration curve of Cd(II) for (a), Pb(II) for (b) and Cr(VI) for (c) of Contact time optimization.

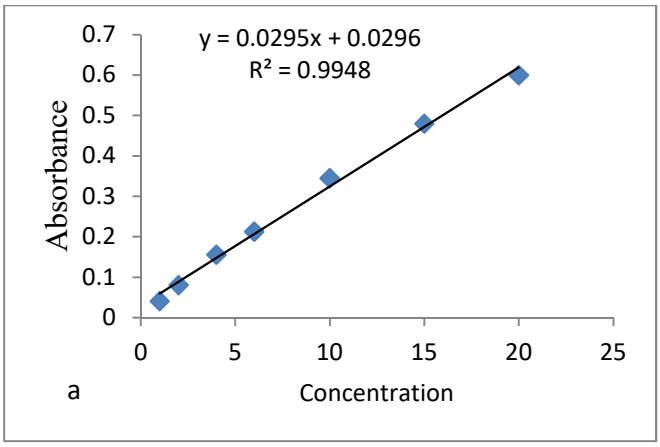

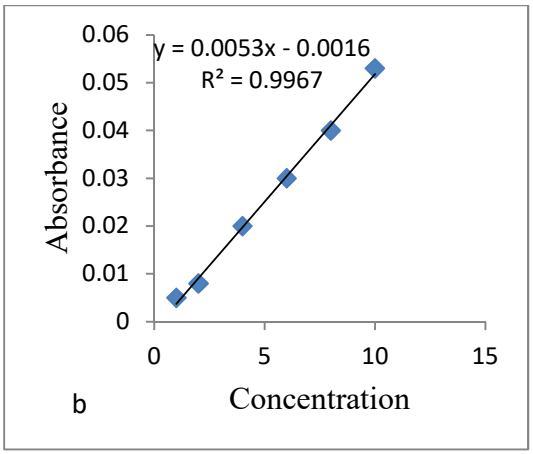

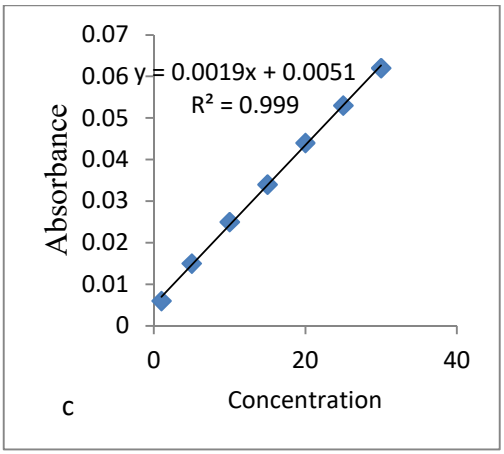

Appendix Figure **5**. Calibration curve of Cd(II) for (a), Pb(II) for (b) and Cr(VI) for (c) of agitation speed optimization.

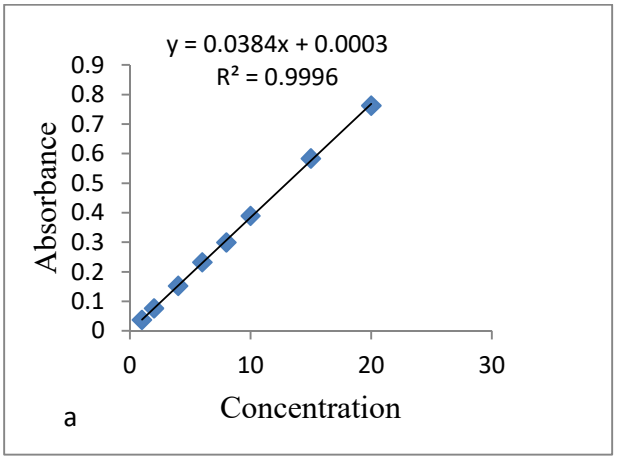

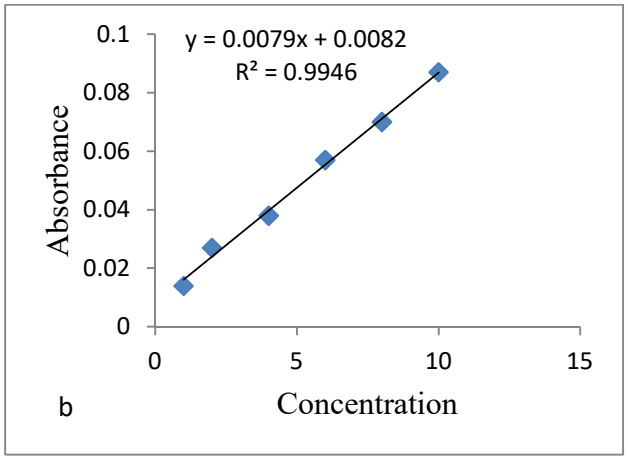

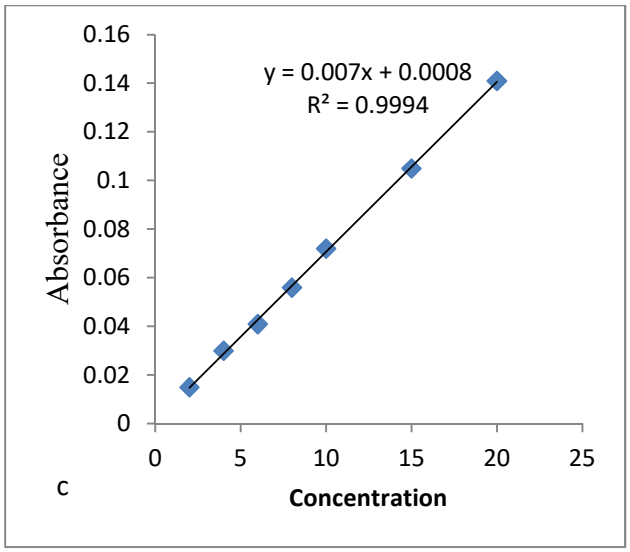

Appendix Figure 6. Calibration curve of Cd(II) for (a), Pb(II) for (b) and Cr(VI) for (c) of Effect of concentration ion optimization.

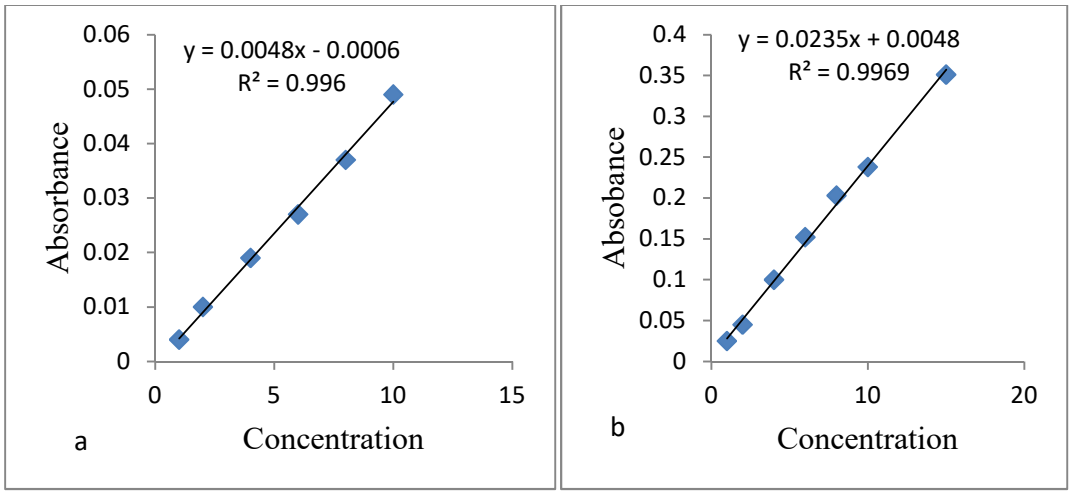

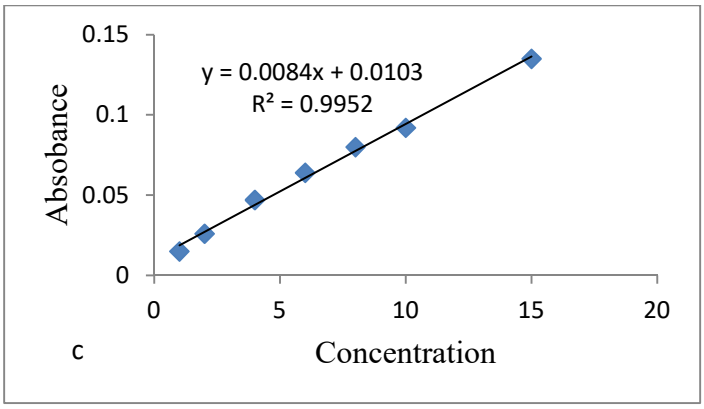

Appendix Figure 7. Calibration curve of Cd(II) for (a), Pb(II) for (b) and Cr(VI) for (c) of Effect of ion interference.

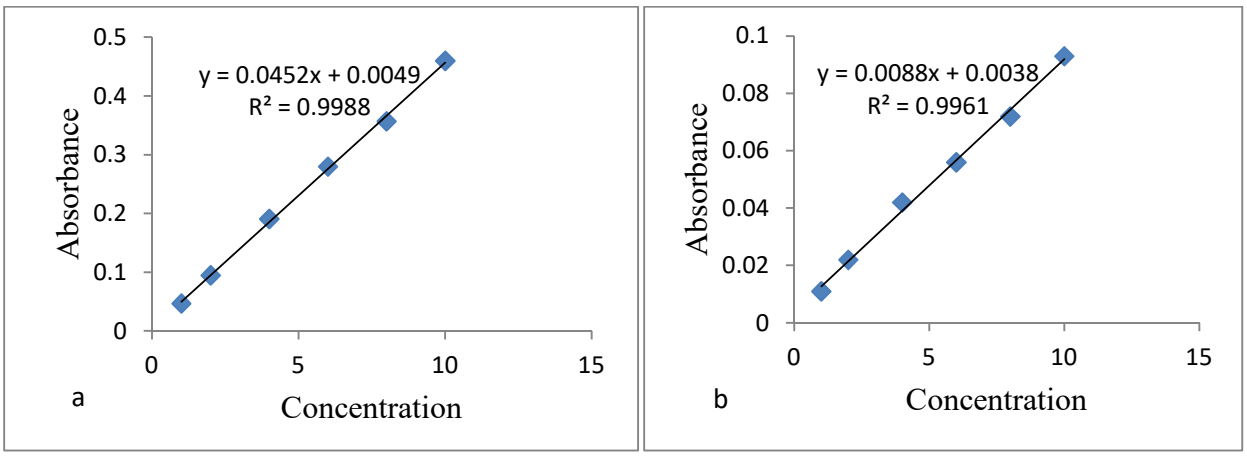

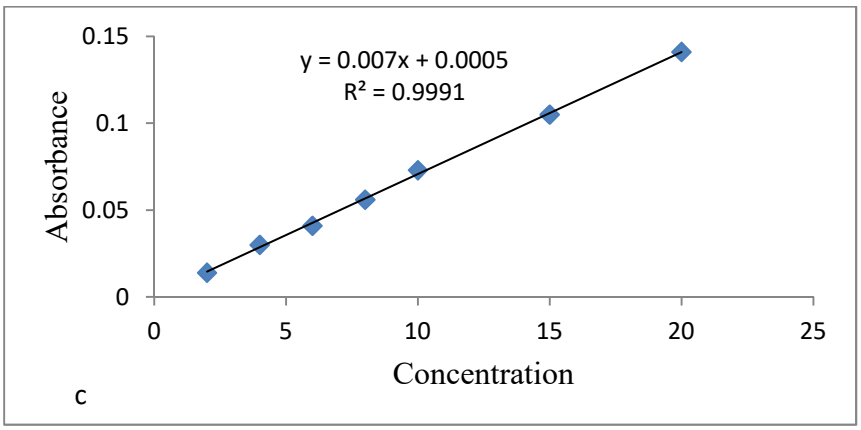

Appendix Figure 8. Calibration curve of Cd(II) for (a), Pb(II) for (b) and Cr(VI) for (c) of Thermodynamic study.

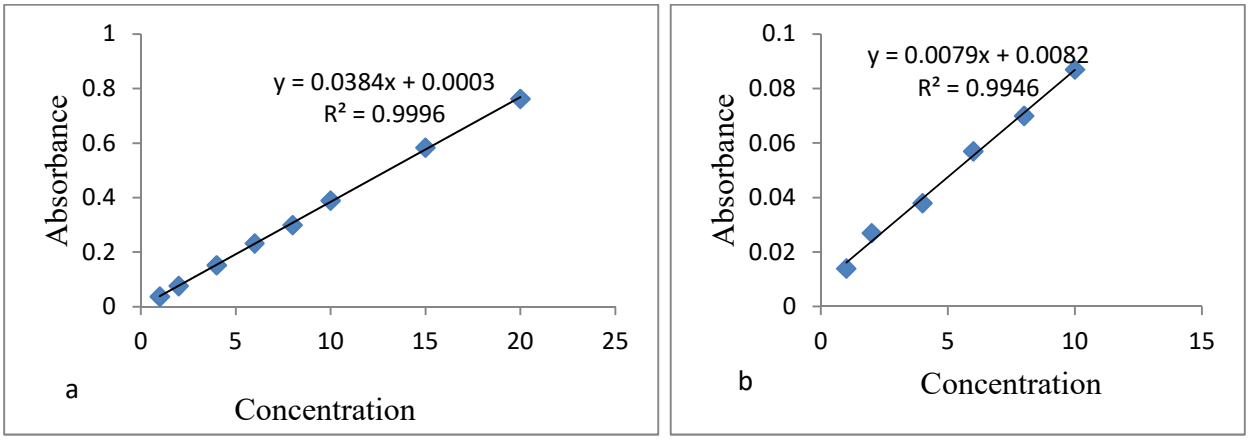

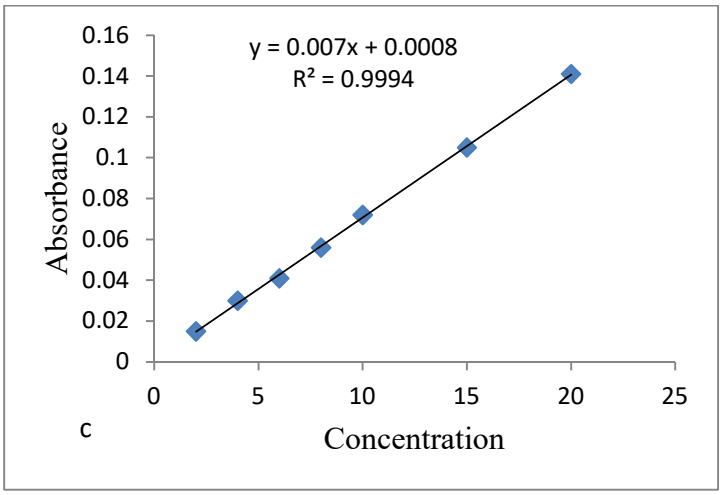

Appendix Figure 9. Calibration curve of Cd(II) for (a), Pb(II) for (b) and Cr(VI) for (c) of kinetic study.